Article
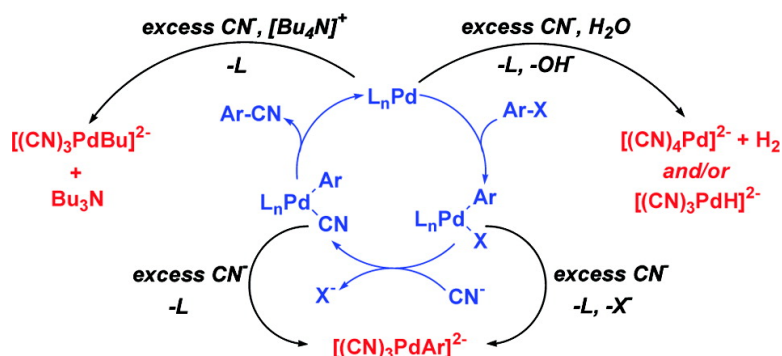
Mechanisms of Catalyst Poisoning in Palladium-Catalyzed Cyanation of Haloarenes. Remarkably Facile C–N Bond Activation in the [(PhP)Pd]/[BuN] CN System

Stefan Erhardt, Vladimir V. Grushin, Alison H. Kilpatrick, Stuart
A. Macgregor, William J. Marshall, and D. Christopher Roe

More About This Article

Additional resources and features associated with this article are available within the HTML version:

- Supporting Information
- Links to the 4 articles that cite this article, as of the time of this article download
- Access to high resolution figures
- Links to articles and content related to this article
- Copyright permission to reproduce figures and/or text from this article

View the Full Text HTML

Mechanisms of Catalyst Poisoning in Palladium-Catalyzed Cyanation of Haloarenes. Remarkably Facile C−N Bond Activation in the [(Ph₃P)₄Pd]/[Bu₄N]⁺ CN⁻ System

Stefan Erhardt,[‡] Vladimir V. Grushin,*,[†] Alison H. Kilpatrick,[‡] Stuart A. Macgregor,*,[‡] William J. Marshall,[†] and D. Christopher Roe[†]

Central Research & Development, E. I. DuPont de Nemours and Co., Inc., Experimental Station, Wilmington, Delaware 19880, and School of Engineering and Physical Sciences, William H. Perkin Building, Heriot-Watt University, Edinburgh EH14 4AS, U.K.

Received October 30, 2007; E-mail: vlad.grushin-1@usa.dupont.com; s.a.macgregor@hw.ac.uk

Abstract: Reaction paths leading to palladium catalyst deactivation during cyanation of haloarenes (eq 1) have been identified and studied. Each key step of the catalytic loop (Scheme 1) can be disrupted by excess cyanide, including ArX oxidative addition, X/CN exchange, and ArCN reductive elimination. The catalytic reaction is terminated via the facile formation of inactive $[(CN)_4Pd]^{2-}$, $[(CN)_3PdH]^{2-}$, and $[(CN)_3PdAr]^{2-}$. Moisture is particularly harmful to the catalysis because of facile CN^- hydrolysis to HCN that is highly reactive toward Pd(0). Depending on conditions, the reaction of $[(Ph_3P)_4Pd]$ with HCN in the presence of extra CN^- can give rise to $[(CN)_4Pd]^{2-}$ and/or the remarkably stable new hydride $[(CN)_3PdH]^{2-}$ (NMR, X-ray). The X/CN exchange and reductive elimination steps are vulnerable to excess CN^- because of facile phosphine displacement leading to stable $[(CN)_3PdAr]^{2-}$ that can undergo ArCN reductive elimination only in the absence of extra CN^-. When a quaternary ammonium cation such as $[Bu_4N]^+$ is used as a phase-transfer agent for the cyanation reaction, C−N bond cleavage in the cation can occur via two different processes. In the presence of trace water, CN^- hydrolysis yields HCN that reacts with Pd(0) to give $[(CN)_3PdH]^{2-}$. This also releases highly active OH^- that causes Hofmann elimination of $[Bu_4N]^+$ to give Bu_3N, 1-butene, and water. This decomposition mode is therefore catalytic in H_2O. Under anhydrous conditions, the formation of a new species, $[(CN)_3PdBu]^{2-}$, is observed, and experimental studies suggest that electron-rich mixed cyano phosphine Pd(0) species are responsible for this unusual reaction. A combination of experimental (kinetics, labeling) and computational studies demonstrate that in this case C−N activation occurs via an S_N2-type displacement of amine and rule out alternative 3-center C−N oxidative addition or Hofmann elimination processes.

Introduction

One of the most efficient modern synthetic routes to aromatic nitriles is palladium-catalyzed cyanation of the corresponding haloarenes (eq 1).[1] The cyano group is an important functionality[2] in numerous intermediates, dyes, pharmaceuticals, and agrochemicals.[1,2] A serious drawback of the catalytic cyanation method is the low tolerance of palladium catalysts to excess cyanide, one of the two key reagents, in the liquid phase. This problem has been widely recognized[1] since the discovery of aromatic cyanation, catalyzed by palladium[3] and nickel[4]

complexes, and recently reconfirmed in a targeted research report.[5]

$$\text{Ar–X} + \text{CN}^- \xrightarrow{\text{Pd catalyst}} \text{Ar–CN} + \text{X}^- \qquad (1)$$
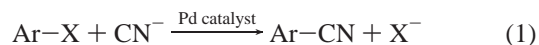
The mechanism of palladium catalyst poisoning during the cyanation process (eq 1) needs to be understood to develop methods to avoid or suppress the catalyst deactivation. Although it has been found that $Zn(CN)_2$[6] and $K_4[Fe(CN)_6]$[7] are less toxic to the catalyst than KCN and NaCN, very little is known about how the process is terminated by excess cyanide and the factors

[†] DuPont CR&D.

[‡] Heriot-Watt University.

(1) For a recent review, see: Sundermeier, M.; Zapf, A.; Beller, M. *Eur. J. Inorg. Chem.* **2003**, 3513.

(2) Collier, S. J.; Langer, P. *Sci. Synth.* **2004**, *19*, 403.

(3) (a) Takagi, K.; Okamoto, T.; Sakakibara, Y.; Oka, S. *Chem. Lett.* **1973**, 471. (b) Sekiya, A.; Ishikawa, N. *Chem. Lett.* **1975**, 277. (c) Takagi, K.; Okamoto. T.; Sakakibara, Y.; Ohno, A.; Oka, S.; Hayama, N. *Bull. Chem. Soc. Jpn.* **1975**, *48*, 3298. (d) Takagi, K.; Okamoto. T.; Sakakibara, Y.; Ohno, A.; Oka, S.; Hayama, N. *Bull. Chem. Soc. Jpn.* **1976**, *49*, 3177. (e) Akita, Y.; Shimazaki, M.; Ohta, A. *Synthesis* **1981**, 974. (f) Takagi, K.; Sasaki, K.; Sakakibara, Y. *Bull. Chem. Soc. Jpn.* **1991**, *64*, 1118.

(4) (a) Cassar, L. *J. Organomet. Chem.* **1973**, *54*, C57. (b) Cassar, L.; Ferrara, S.; Foa, M. *Adv. Chem. Ser.* **1974**, *132*, 252. (c) Cassar, L.; Foa, M.; Montanari, F.; Marinelli, G. P. *J. Organomet. Chem.* **1979**, *173*, 335. (d) Sakakibara, Y.; Okuda, F.; Shimobayashi, A.; Kirino, K.; Sakai, M.; Uchino, N.; Takagi, K. *Bull. Chem. Soc. Jpn.* **1988**, *61*, 1985. (e) Takagi, K.; Sakakibara, Y. *Chem. Lett*. **1989**, 1957. (f) Sasaki, K.; Sakai, M.; Sakakibara, Y.; Takagi, K. *Chem. Lett*. **1991**, 2017. (g) Sakakibara, Y.; Ido, Y.; Sasaki, K.; Saki, M.; Uchino, N. *Bull. Chem. Soc. Jpn.* **1993**, *66*, 2776. (h) Sakakibara, Y.; Sasaki, K.; Okuda, F.; Hokimoto, A.; Ueda, T.; Sakai, M.; Takagi, K. *Bull. Chem. Soc. Jpn.* **2004**, *77*, 1013.

(5) Marcantonio, K. M.; Frey, L. F.; Liu, Y.; Chen, Y.; Strine, J.; Phenix, B.; Wallace, D. J.; Chen, C-y. *Org. Lett.* **2004**, *6*, 3723.

Scheme 1
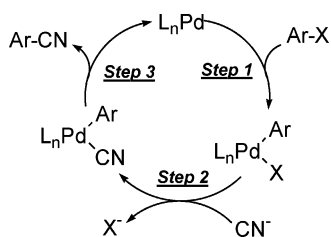
Scheme 2

that may influence the poisoning. In 2003, Beller and co-workers[8] reported that $[Bu_4N]^+$ CN^- impeded the ability of $[(Ph_3P)_4Pd]$ to undergo oxidative addition of the aryl halide substrate in the first step of the process (Scheme 1). A recent preliminary communication by some of us[9] shows that every key step of the catalytic loop may be affected by excess cyanide in solution. In particular, it was demonstrated that the key σ-aryl palladium halide intermediate takes the desired path to ArCN if treated with only 1 equiv of cyanide (steps 2 and 3 in Scheme 1) but is easily converted to stable, catalytically inactive $[(CN)_3PdAr]^{2-}$ in the presence of excess cyanide (Scheme 2). Although the dianion $[(CN)_3PdPh]^{2-}$ may be rendered catalytically active via Ph−CN reductive elimination to give Pd(0) species,[10,11] this process apparently occurs from a tricoordinate complex and thus requires predissociation of one of the Pd−CN bonds.[9] This bond ionization, however, is most efficiently inhibited by even small quantities of extra free cyanide, which shifts the equilibrium between $[(CN)_3PdPh]^{2-}$ and $[(CN)_2PdPh]^-$ toward the unreactive 4-coordinate species.

The preliminary study has also led to identification of yet another reaction that may result in palladium catalyst deactivation if the cyanation process (eq 1) is carried out in the presence of a quaternary alkylammonium salt as a phase transfer catalyst. It was found that $[(Ph_3P)_4Pd]$ readily reacts with $[Bu_4N]^+$ CN^- in THF at room temperature to produce catalytically inactive $[(CN)_3PdH]^{2-}$ (eq 2).
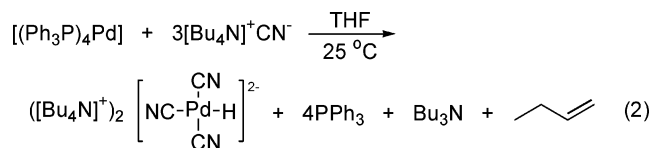

In this article, we describe further critical insights into the mechanisms of palladium catalyst poisoning during aromatic cyanation. In particular, we show that the formation of
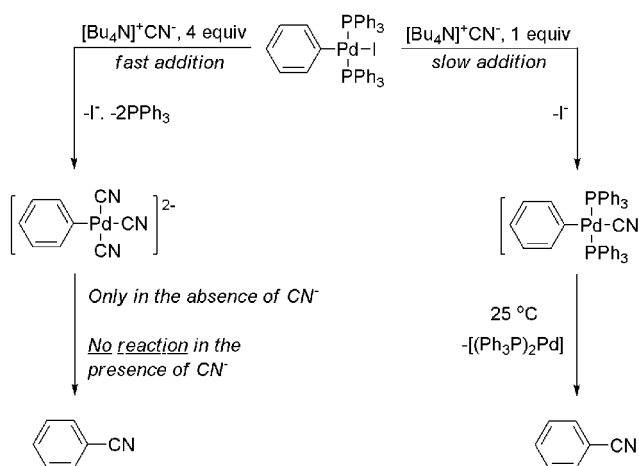
$[(CN)_3PdH]^{2-}$ is linked to the presence of trace water in the reaction system. Under strictly anhydrous conditions, however, a new process leading to the formation of $[(CN)_3PdBu]^{2-}$ has been identified (eq 3). This reaction is a rare example of intermolecular nonallylic single C−N bond activation with a platinum group metal complex.[12−16] We also present a computational study of the mechanism of this unusual C−N activation reaction displayed by the $[(Ph_3P)_4Pd]/[Bu_4N]^+$ CN^- system.
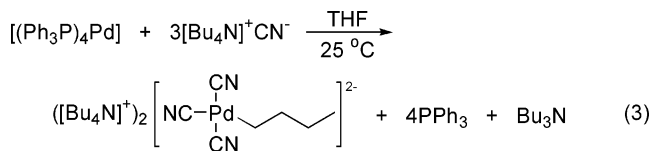
Experimental Studies

C−N Activation in the $[(Ph_3P)_4Pd]/[Bu_4N]^+$ CN^- System. The Formation of $[(CN)_3PdH]^{2-}$ and $[(CN)_3PdBu]^{2-}$. As preliminarily communicated,[9] adding $[Bu_4N]^+$ CN^- to $[(Ph_3P)_4Pd]$ in dry THF resulted in an immediate color change from
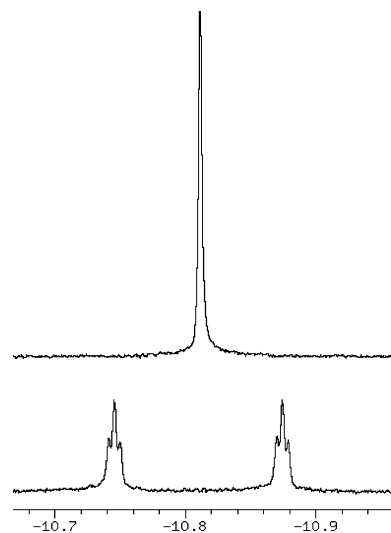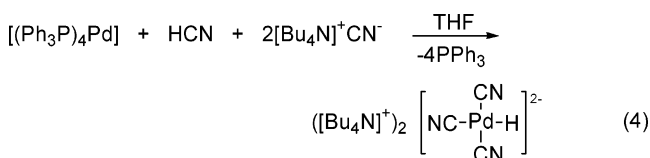
(6) Tschaen, D. M.; Desmond, R.; King, A. O.; Fortin, M. C.; Pipik, B.; King, S.; Verhoeven, T. R. *Synth. Commun.* **1994**, *24*, 887. Since the appearance of this communication, numerous reports have been published, describing the successful use of $Zn(CN)_2$ as the source of cyanide for palladium-catalyzed aromatic cyanation.

(7) Schareina, T.; Zapf, A.; Beller, M. *Chem. Commun.* **2004**, 1388. Schareina, T.; Zapf, A.; Mägerlein, W.; Müller, N.; Beller, M. *Tetrahedron Lett.* **2007**, *48*, 1087. Pinto, A.; Jia, Y.; Neuville, L.; Zhu, J. *Chem.−Eur. J.* **2007**, *13*, 961. Cheng, Yi-n.; Duan, Z.; Li, T.; Wu, Y. *Synlett* **2007**, 543. Zhu, Y.-Z.; Cai, C. *Eur. J. Org. Chem.* **2007**, 2401. Polshettiwar, V.; Hesemann, P.; Moreau, J. J. E. *Tetrahedron* **2007**, *63*, 6784. Cheng, Yi-n.; Duan, Z.; Li, T.; Wu, Y. *Lett. Org. Chem.* **2007**, *4*, 352.

(8) Sundermeier, M.; Zapf, A.; Mutyala, S.; Baumann, W.; Sans, J.; Weiss, S.; Beller, M. *Chem.−Eur. J.* **2003**, *9*, 1828.

(9) Dobbs, K. D.; Marshall, W. J.; Grushin, V. V. *J. Am. Chem. Soc.* **2007**, *129*, 30.

(10) For a recent review of reductive elimination from Pd(II), see: Hartwig, J. F. *Inorg. Chem.* **2007**, *46*, 1936.

(11) For studies of R−CN reductive elimination from Pd(II), see: Marcone, J. E.; Moloy, K. G. *J. Am. Chem. Soc.* **1998**, *120*, 8527. Huang, J.; Haar, C. M.; Nolan, S. P.; Marcone, J. E.; Moloy, K. G. *Organometallics* **1999**, *18*, 297.

(12) Allylic C−N activation with late transition metals is more common, apparently due to C=C bond precoordination prior to C−N bond cleavage. For a review of the synthetic use of palladium π-allyl methodology to cleave the C−N bond of allylamines, see: Guibe, F. *Tetrahedron* **1998**, *54*, 2967.

(13) For selected recent reports on metal-assisted allylic C−N bond cleavage, see: (a) Alcaide, B.; Almendros, P.; Alonso, J. M. *Chem.−Eur. J.* **2006**, *12*, 2874. (b) Cadierno, V.; Garcia-Garrido, S. E.; Gimeno, J.; Nebra, N. *Chem. Commun.* **2005**, 4086. (c) Alcaide, B.; Almendros, P.; Alonso, J. M.; Luna, A. *Synthesis* **2005**, 668. (d) Escoubet, S.; Gastaldi, S.; Bertrand, M. *Eur. J. Org. Chem.* **2005**, 3855. (e) Alcaide, B.; Almendros, P.; Alonso, J. M. *Chem.−Eur. J.* **2003**, *9*, 5793. (f) Aresta, M.; Quaranta, E. *J. Organomet. Chem.* **2002**, *662*, 112. (g) Torrent, M.; Musaev, D. G.; Morokuma, K. *Organometallics* **2000**, *19*, 4402. (h) Aresta, M.; Quaranta, E.; Dibenedetto, A.; Giannoccaro, P.; Tommasi, I.; Lanfranchi, M.; Tiripicchio, A. *Organometallics* **1997**, *16*, 834.

(14) For chelation-assisted and pincer complex C−N bond activation, see: Takano, K.; Inagaki, A.; Akita, M. *Chem. Lett.* **2006**, *35*, 434. Weng, W.; Guo, C.; Moura, C.; Yang, L.; Foxman, B. M.; Ozerov, O. V. *Organometallics* **2005**, *24*, 3487. Ozerov, O. V.; Guo, C.; Fan, L.; Foxman, B. M. *Organometallics* **2004**, *23*, 5573. Fan, L.; Yang, L.; Guo, C.; Foxman, B. M.; Ozerov, O. V. *Organometallics* **2004**, *23*, 4778. Yamamoto, Y.; Seta, J.; Murooka, H.; Han, X.-H. *Inorg. Chem. Commun.* **2003**, *6*, 202. Morilla, M. E.; Morfes, G.; Nicasio, M. C.; Belderrain, T. R.; Diaz-Requejo, M. M.; Graiff, C.; Tiripicchio, A.; Sanchez-Delgado, R.; Perez, P. J. *Chem. Commun.* **2002**, *17*, 1848. Gandelman, M.; Milstein, D. *Chem. Commun.* **2000**, *17*, 1603.

(15) For C−N activation in N-heterocyclic carbene complexes, see: Burling, S.; Mahon, M. F.; Powell, R. E.; Whittlesey, M. K.; Williams, J. M. J. *J. Am. Chem. Soc.* **2006**, *128*, 13702. Caddick, S.; Cloke, F. G. N.; Hitchcock, P. B.; de K. Lewis, A. K. *Angew. Chem., Int. Ed.* **2004**, *43*, 5824.

(16) Suzuki coupling reactions of aryltrimethylammonium,[16a] vinyltrimethyl-ammonium,[16b] and N-vinylpyridinium salts have been recently reported. (a) Blakey, S. B.; MacMillan, D. W. C. *J. Am. Chem. Soc.* **2003**, *125*, 6046. (b) Buszek, K. R.; Brown, N. *Org. Lett.* **2007**, *9*, 707.

yellow to tan, followed by gradual loss of color. After several hours, a colorless reaction mixture was produced, which contained $([Bu_4N]^+)_2 [(CN)_3Pd(H)]^{2-}$, PPh_3, Bu_3N, and 1-butene, as shown in eq 2. The formation of a biphasic liquid−liquid system was frequently observed toward the end of the reaction, due to phase segregation of the ionic hydride, a viscous colorless oil that is only moderately soluble in THF at room temperature. Monophasic reaction mixtures were obtained at higher dilution.

After this first round of studies, we continued our research toward a better understanding of the mechanism of this unusual reaction. By then, our supplies of the Pd(0) complex had been exhausted and hence the project was continued with a new sample of $[(Ph_3P)_4Pd]$ (99.9+%) freshly purchased from Strem. To our surprise, the first experiments with the new $[(Ph_3P)_4Pd]$ reagent resulted in a slightly different outcome. Whereas the initial visual signs of the reaction were similar, the resulting mixture retained homogeneity and exhibited no phase segregation, even though the ionic hydride was expected to oil out. The ^1H and ^{31}P NMR spectra of the reaction mixture indicated the presence of free PPh_3 and Bu_3N, as before. However, only small quantities of the hydride $[(CN)_3PdH]^{2-}$ (<10%) and 1-butene were formed, if any. Instead, a new species, $[(CN)_3PdBu]^{2-}$, appeared to be the main product of the reaction (eq 3). By comparing eqs 2 and 3, one can see that the stoichiometry of the two reactions is the same, except that the old $[(Ph_3P)_4Pd]$ sample reacted to produce $[(CN)_3PdH]^{2-}$ and 1-butene separately (eq 2), whereas these two molecules came together to form $[(CN)_3PdBu]^{2-}$ (eq 3) when the newly purchased $[(Ph_3P)_4Pd]$ was used. The above observations prompted us to investigate the apparently erratic $[(Ph_3P)_4Pd]/[Bu_4N]^+ CN^-$ system in more detail, using both experimental and computational methods. These studies have defined a major route for palladium catalyst deactivation in the presence of water, even in trace quantities, and ultimately this may prove to be the most common mechanism undermining catalytic aromatic cyanation. For our experimental work, we needed to devise routes to obtain pure samples of salts of both $[(CN)_3PdH]^{2-}$ and $[(CN)_3PdBu]^{2-}$.

Preparation, Isolation, and Characterization of Salts of $[(CN)_3PdH]^{2-}$. An independent synthetic method was developed for $[(CN)_3PdH]^{2-}$. Slow addition of a dilute THF solution of aqueous $H^{13}CN$ to $[(Ph_3P)_4Pd]$ in the presence of ca. 2.1 equiv of $[Bu_4N]^+ {}^{13}CN^-$ in THF afforded $([Bu_4N]^+)_2 [(^{13}CN)_3PdH]^{2-}$ in high yield (eq 4). As mentioned above, this tetrabutylammonium salt is an oil that partially precipitated out of the reaction solution. Our previous attempts to obtain an accurate crystal structure of this hydride as its PPN salt (PPN$^+$ = [Ph₃-PNPPh₃]$^+$) were unsuccessful due to disorder.[9] In the present work, we found that reacting $([Bu_4N]^+)_2 [(^{13}CN)_3PdH]^{2-}$ with $[Et_4N]^+ BF_4^-$ in a THF−acetonitrile mixture resulted in precipitation of solid $([Et_4N]^+)_2 [(^{13}CN)_3PdH]^{2-}$ which was isolated in an analytically pure form in 90% yield and fully characterized in solution and in the solid state. The Pd−H resonance at −10.8 ppm (Figure 1) appears as a doublet of triplets due to the coupling to one trans and two cis ^{13}C nuclei

$$[(Ph_3P)_4Pd] + HCN + 2[Bu_4N]^+CN^- \xrightarrow[-4PPh_3]{THF}$$

$$([Bu_4N]^+)_2 \left[\begin{array}{c} CN \\ | \\ NC-Pd-H \\ | \\ CN \end{array} \right]^{2-} \quad (4)$$

Figure 1. ^1H (bottom) and $^1H\{^{13}C\}$ (top) NMR spectra of $[(^{13}CN)_3Pd(H)]^{2-}$ ($trans\text{-}J_{C-H} = 64.9$ Hz, $cis\text{-}J_{C-H} = 2.6$ Hz) in CD_3CN.
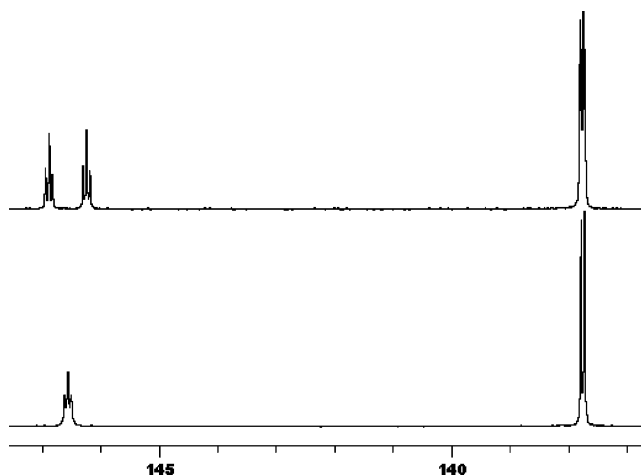
Figure 2. ^{13}C (top) and $^{13}C\{^1H\}$ (bottom) NMR spectra of $[(^{13}CN)_3Pd(H)]^{2-}$ ($J_{C-C} = 5.8$ Hz; $trans\text{-}J_{C-H} = 64.9$ Hz, $cis\text{-}J_{C-H} = 2.6$ Hz) in CD_3CN.

with $J_{C-H} = 64.9$ and 2.6 Hz, respectively. This signal was observed as a singlet when the spectrum was acquired ^{13}C-decoupled (Figure 1). In full accord, a doublet and a triplet with $J_{C-C} = 5.8$ Hz appeared in the $^{13}C\{^1H\}$ NMR spectrum of the hydride, and both C−H coupling constants were observed with the ^1H-decoupler off (Figure 2).[17]

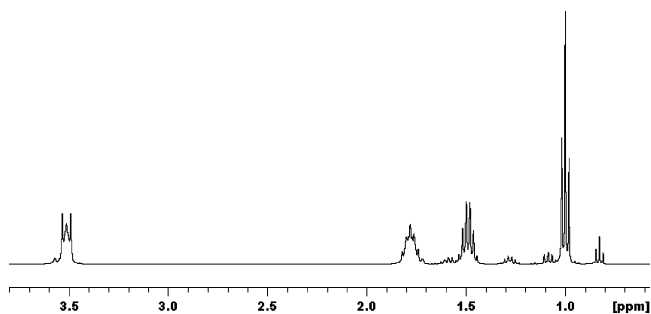A highly accurate X-ray structure of $([Et_4N]^+)_2 [(^{13}CN)_3PdH]^{2-}$ (Figure 3) exhibited no signs of disorder in the crystal, possibly due to hydrogen bonding interactions of the cyano ligands on palladium with the C−H bonds of the cation (for the CIF file, see the Supporting Information). The hydride ligand was located from a difference map and fully refined. The Pd−H bond distance (1.61 Å) appears to be the longest in the small family of structurally characterized terminal palladium hydrides.[18,19] This points to the strong trans influence of the cyano ligand, although this is not as large as that of hydride, the mutually trans Pd-C1/C3 bonds (1.996(2) Å and 2.000(2) Å, respectively) being noticeably shorter than Pd−C2 trans to hydride (2.053-(2) Å). Considering the well-known poor stability of molecular palladium hydrides,[18] the dianion $[(^{13}CN)_3PdH]^{2-}$ is remarkably stable (see below), despite its long Pd−H bond.

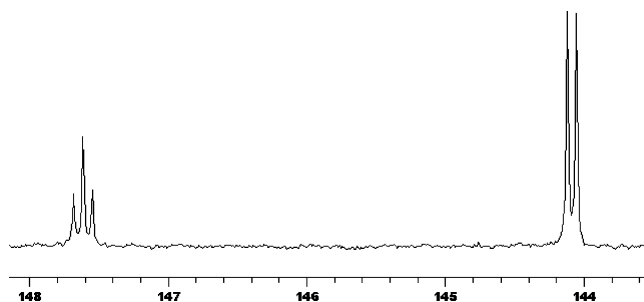**Formation and Characterization of $[(CN)_3PdBu]^{2-}$.** The n-butyl complex $([Bu_4N]^+)_2 [(^{13}CN)_3PdBu]^{2-}$ was prepared by
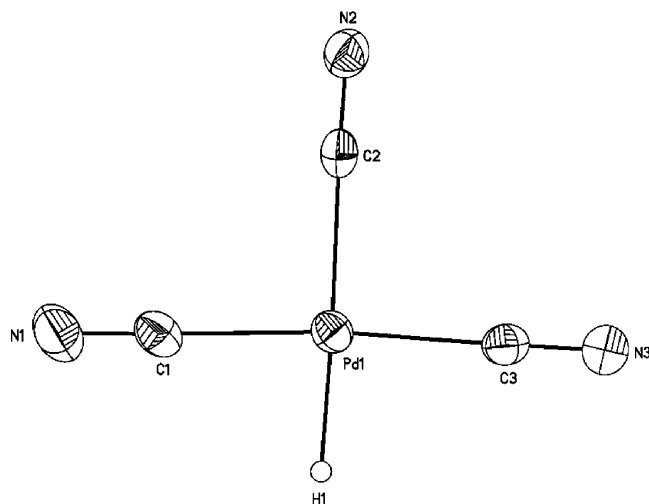
Figure 3. ORTEP drawing of the palladium hydride dianion of ([Et$_4$N]$^+$)$_2$ [(^{13}CN)$_3$PdH]$^{2-}$ with thermal ellipsoids drawn to the 50% probability level. Selected bond distances (Å) and bond angles (deg): Pd(1)−H(1) 1.61, Pd-(1)−C(1) 1.996(2), Pd(1)−C(3) 2.000(2), Pd(1)−C(2) 2.053(2), N(1)−C(1) 1.150(2), N(2)−C(2) 1.150(2), N(3)−C(3) 1.149(2), C(1)−Pd(1)−C(3) 174.98(7), C(1)−Pd(1)−C(2) 93.11(7), C(3)−Pd(1)−C(2) 91.91(6).

Figure 4. ^{1}H NMR spectrum of ([Bu$_4$N]$^+$)$_2$ [(CN)$_3$PdBu]$^{2-}$ in THF-d_8. The low-intensity resonances at 1.7 and 3.6 ppm are residual solvent peaks.

Figure 5. ^{13}C{^{1}H} NMR spectrum of [(^{13}CN)$_3$PdBu]$^{2-}$ (J_{C-C} = 6.8 Hz) in THF-d_8.

treating the newly purchased [(Ph$_3$P)$_4$Pd] with [Bu$_4$N]$^+$ ^{13}CN$^-$ in dry THF or benzene. This reaction (eq 3) was found to proceed faster at *lower* concentrations of [(Ph$_3$P)$_4$Pd], in full accord with the results of our subsequent kinetic studies (see below). At ambient temperature and [[(Ph$_3$P)$_4$Pd]] = 0.5−1.5 × 10^{-2} mol dm^{-3}, it took the reaction 1−3 days to go to completion, whereas for [[(Ph$_3$P)$_4$Pd]] = ca. 8 × 10^{-2} mol dm^{-3} and higher virtually no reaction was observed. The resulting complex ([Bu$_4$N]$^+$)$_2$ [(^{13}CN)$_3$PdBu]$^{2-}$ is a viscous oil that is easily soluble in THF and MeCN but insoluble in benzene and ether. Attempts to isolate the solid [Et$_4$N]$^+$ salt using [Et$_4$N]$^+$ CN$^-$ in an analogous fashion to that employed for [(^{13}CN)$_3$PdH]$^{2-}$ failed as a result of the greater solubility of the complex containing the more lipophilic Pd−Bu moiety. Instead, precipitation of [Et$_4$N]$^+$ CN$^-$ was seen (NMR, X-ray; Supporting Information). Therefore, ([Bu$_4$N]$^+$)$_2$ [(^{13}CN)$_3$PdBu]$^{2-}$ could only be characterized in solution. The ^{1}H NMR spectrum of isolated ([Bu$_4$N]$^+$)$_2$ [(^{13}CN)$_3$PdBu]$^{2-}$ (Figure 4) displays eight multiplets arising from the *n*-butyl groups of two different types, whereas a doublet (144.1 ppm) and a triplet (147.6 ppm) with J_{C-C} = 6.8 Hz were observed in the ^{13}C NMR spectrum of a ^{13}CN labeled sample (Figure 5). These ^{13}C NMR chemical shifts are

(17) The preliminary experiments^9 with ^{13}C-enriched cyanide were carried out with the already new Strem 99.9+% reagent that was reacted with [Bu$_4$N]$^+$ ^{13}CN$^-$ to give small yet ^{1}H NMR-detectable quantities of the hydride. Because in the ^{1}H NMR spectrum the doublet of triplets (1H, Pd-H) integrated against the aromatic protons (40H, PPh$_3$) as ca. 0.6 to 40, it was concluded that the ^{13}C NMR signals at 144.6 and 148.0 ppm observed for the same reaction solution were from the hydrido species, [(^{13}CN)$_3$PdH]$^{2-}$, whereas in fact those were from [(CN)$_3$PdBu]$^{2-}$, the main product of the reaction. The big ^{1}H NMR integration error is yet another reminder that one should be careful when quantifying a weak MH multiplet resonance against CH signals of much higher intensity.
(18) Grushin, V. V. *Chem. Rev.* **1996**, *96*, 2011.
(19) Clement, N. D.; Cavell, K. J.; Jones, C.; Elsevier, C. J. *Angew. Chem., Int. Ed.* **2004**, *43*, 1277. Perez, P. J.; Calabrese, J. C.; Bunel, E. E. *Organometallics* **2001**, *20*, 337. Wander, S. A.; Miedaner, A.; Noll, B. C.; Barkley, R. M.; DuBois, D. L. *Organometallics* **1996**, *15*, 3360. Leoni, P.; Sommovigo, M.; Pasquali, M.; Midollini, S.; Braga, D.; Sabatino, P. *Organometallics* **1991**, *10*, 1038. Di Bugno, C.; Pasquali, M.; Leoni, P.; Sabatino, P.; Braga, D. *Inorg. Chem.* **1989**, *28*, 1390. Young, S. J.; Kellenberger, B.; Reibenspies, Joseph H.; Himmel, S. E.; Manning, M.; Anderson, O. P.; Stille, J. K. *J. Am. Chem. Soc.* **1988**, *110*, 5744. Braga, D.; Sabatino, P.; Di Bugno, C.; Leoni, P.; Pasquali, M. *J. Organomet. Chem.* **1987**, *334*, C46.

both concentration and solvent dependent. Unambiguous NMR identification and characterization of the *n*-butyl palladium complex and Bu$_3$N, the other reaction product, was carried out using a combination of TOCSY and HMBC, and was facilitated by the use of [(CH$_3$CH$_2$CD$_2$CH$_2$)$_4$N]$^+$ ^{13}CN$^-$ to alleviate ^{1}H spectral overlap (see Experimental Section). These studies confirmed the remarkable selectivity toward the formation of only the linear, *n*-butyl palladium isomer and indicated that no deuterium scrambling occurred during the reaction.

The Dianions [(CN)$_3$PdH]$^{2-}$ and [(CN)$_3$PdBu]$^{2-}$ are not Interconvertible under the Reaction Conditions. One might expect the dianions [(CN)$_3$PdH]$^{2-}$ and [(CN)$_3$PdBu]$^{2-}$ to be interconvertible via migratory insertion of 1-butene into the Pd−H bond and β-elimination from the *n*-butyl ligand. If these transformations were feasible, the selectivity toward the formation of [(CN)$_3$PdH]$^{2-}$ and [(CN)$_3$PdBu]$^{2-}$ (eqs 2 and 3) could, in principle, be affected by factors favoring or precluding olefin removal from the system. Independent experiments, however, pointed to a striking reluctance of [(CN)$_3$PdH]$^{2-}$ and [(CN)$_3$-PdBu]$^{2-}$ to interconvert in THF in the presence of 0.03−1 equiv of extra cyanide in the form of [Bu$_4$N]$^+$ CN$^-$. Heating the isolated ([Bu$_4$N]$^+$)$_2$ [(^{13}CN)$_3$PdBu]$^{2-}$ in THF in the presence of only 5% of [Bu$_4$N]$^+$ ^{13}CN$^-$ at 60 °C for 3 h resulted in no change. Likewise, no transformation was observed upon treatment of ([Bu$_4$N]$^+$)$_2$ [(^{13}CN)$_3$PdH]$^{2-}$ with 1-butene in THF containing ca. 1−5% of [Bu$_4$N]$^+$ ^{13}CN$^-$ first at room temperature and then at 55 °C for 5 h.^{20a} Thus, once formed [(CN)$_3$PdH]$^{2-}$ and/or [(CN)$_3$PdBu]$^{2-}$ do not interconvert, and this is in accord with the selective formation of the *n*-butyl palladium isomer and the lack of deuterium scrambling in the reaction of [(CH$_3$CH$_2$CD$_2$CH$_2$)$_4$N]$^+$ ^{13}CN$^-$ with [(Ph$_3$P)$_4$Pd] (see above). Finally, the formation of only [(CN)$_3$PdBu]$^{2-}$ and no NMR-detectable quantities of the hydride were observed when the reaction of the new [(Ph$_3$P)$_4$Pd] with [Bu$_4$N]$^+$ ^{13}CN$^-$ was

repeated at room temperature and with vigorous stirring in a flame-dried glass tube that was flame-sealed *under vacuum* (<0.001 Torr at −196 °C).[20b] This result indicated that the difference in the reaction outcomes between the earlier (eq 2) and more recent (eq 3) experiments cannot be accounted for by the change in the reaction conditions affecting olefin removal from the liquid phase.

The Critical Role of Water in the Selective Formation of $[(CN)_3PdH]^{2-}$ or $[(CN)_3PdBu]^{2-}$. As $[(CN)_3PdBu]^{2-}$ and $[(CN)_3PdH]^{2-}$ were found not to interconvert, the variation in the reaction outcomes (eqs 2 and 3) was apparently caused by some difference between the old and new $[(Ph_3P)_4Pd]$ reagents, because all other chemicals and solvents used throughout this work were the same.[21a] Furthermore, we carried out the reaction of $[Bu_4N]^+ CN^-$ with two other sources of triphenylphosphine Pd(0) complexes: another freshly received commercial sample of $[(Ph_3P)_4Pd]$ (99%; Aldrich) and $[(Ph_3P)_3Pd]$ that was prepared according to the literature.[22] In both cases, the Pd−Bu complex was formed as the main product (eq 3) and only small amounts of the hydride were detected: ca. 5% for the Aldrich reagent and <1% for the prepared $[(Ph_3P)_3Pd]$.

An important result was obtained when the new Strem 99.9+% $[(Ph_3P)_4Pd]$ reagent was treated with $[Bu_4N]^+ CN^-$ in the presence of a small quantity of water (1−5 equiv per palladium) that was deliberately added to the system. In this case, the tan-yellow color that emerged immediately upon mixing the reagents faded much more rapidly, and after a few hours the reaction produced ca. 80% of the *hydride* (eq 2).[21b] Because similar experiments with the same Pd(0) reagent *in the absence of water* always produced the *butyl complex* (eq 3), we propose that the old Pd(0) reagent might have been contaminated with a small amount of water, which could not

be detected in our standard purity tests.[21c] Due to the significant difference in the molecular weights of $[(Ph_3P)_4Pd]$ (MW = 1155) and H_2O (MW = 18), the presence of 1 mol equiv of water in the palladium complex would translate into only ca. 1.5% contamination by weight. As will be discussed in detail below, cyanide is easily hydrolyzed in the presence of water to produce HCN, which rapidly reacts with $[(Ph_3P)_nPd]$ to give $[(CN)_3PdH]^{2-}$ in the presence of $[Bu_4N]^+ CN^-$ (eq 4). This explains why the presence or absence of even small quantities of H_2O can strongly influence the reaction paths for the $[(Ph_3P)_4Pd]/[Bu_4N]^+ CN^-$ system, such that $[(CN)_3PdH]^{2-}$ (eq 2) or $[(CN)_3PdBu]^{2-}$ (eq 3) can be formed predominantly or almost exclusively. Even water absorbed on the walls of the glassware used for the reaction can cause the formation of some quantities of $[(CN)_3PdH]^{2-}$, no matter how dry all the reagents and the solvent are.

Reactivity of $[(Ph_3P)_4Pd]$ toward Cyanide in the Presence of Water and in the Absence of a Quaternary Alkylammonium Cation. As shown above, Pd(0) is highly reactive toward HCN, a weak acid (pKa = ca. 9) that is easily generated upon hydrolysis of the cyanide anion. A series of experiments was designed to explore the reactivity of $[(Ph_3P)_4Pd]$ toward cyanide in the presence of water and in the absence of a noninnocent cation, such as $[Bu_4N]^+$. Stirring a solution of $[(Ph_3P)_4Pd]$ in dry THF with excess $K^{13}CN$ for several hours at room temperature did not result in any reaction. However, once O_2-free D_2O or H_2O (140 equiv per palladium) was added to the mixture, the yellow color from the Pd(0) complex began to fade, and full discoloration was observed within ca. 10 min of agitaton, pointing to the disappearance of Pd(0). Analysis of the reaction mixture indicated the presence of free PPh_3 (^{31}P NMR: s, −5.5 ppm) and $[(^{13}CN)_4Pd]^{2-}$ (^{13}C NMR: s, 131.4 ppm) as the only P- and ^{13}C-containing products. This reaction (eq 5) is an important path leading to catalyst poisoning in palladium-catalyzed cyanation of haloarenes,[1] a process that is seldom run under rigorously anhydrous conditions (see Discussion).

$$[(Ph_3P)_4Pd] + 4KCN + 2H_2O \rightarrow$$
$$K_2[Pd(CN)_4] + 4PPh_3 + 2KOH + H_2 \quad (5)$$
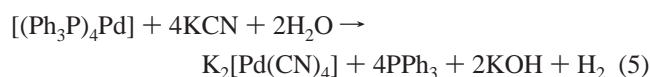
We propose that first the Pd(0) undergoes oxidative addition with the $H^{13}CN$ generated upon the hydrolysis of $K^{13}CN$ to form

(20) (a) It is noteworthy that isolated and purified $([Et_4N]^+)_2 [(^{13}CN)_3PdH]^{2-}$ that is insoluble in THF was found to react with ethylene or 1-butene in *acetonitrile, as long as no extra cyanide was present*. Both reactions occurred within ca. 1 hour at room temperature. The reaction with ethylene produced $[(^{13}CN)_3PdEt]^{2-}$ (^{13}C NMR: 144.6, d, J_{C-C} = 6.8 Hz, 2C; 146.1, t, J_{C-C} = 6.8 Hz, 1C). At the beginning, the reaction with 1-butene gave a ca. 3:2 mixture of two species that we formulate as $[(^{13}CN)_3Pd(n-Bu)]^{2-}$ (^{13}C NMR: 144.4, d, J_{C-C} = 7.0 Hz, 2C; 146.3, t, J_{C-C} = 7.0 Hz, 1C) and $[(^{13}CN)_3Pd(sec-Bu)]^{2-}$ (^{13}C NMR: 145.6, d, J_{C-C} = 7.3 Hz, 2C; 146.9, t, J_{C-C} = 7.3 Hz, 1C). As the reaction proceeded, the *n*-Bu/*sec*-Bu product ratio was quickly increasing to reach ca. 20:1 at thermodynamic equilibrium. This migratory insertion reaction was efficiently shut down by extra cyanide. After a 1:1 mixture of $([Et_4N]^+)_2 [(^{13}CN)_3PdH]^{2-}$ and $[Bu_4N]^+ {}^{13}CN^-$ was dissolved in 1-butene-saturated MeCN, no reaction was observed for 14 days. Simply dissolving pure $([Et_4N]^+)_2 [(^{13}CN)_3PdH]^{2-}$ in MeCN resulted in rapidly self-decelerating decomposition to palladium black, $[(^{13}CN)_4Pd]^{2-}$, free cyanide, and H_2 (^1H NMR: s, 4.6 ppm). The resonance from the H_2 disappeared after another gas, N_2, ethylene, or 1-butene had been bubbled through the solution. The previously described[9] decomposition of $(PPN^+)_2$ $[(CN)_3PdH]^{2-}$ in MeCN occurred similarly, except HCN rather than H_2 was detected among the products. Apparently, in both cases the first step is the reversible ionization of the Pd−CN bond trans to hydride, followed by reductive elimination of HCN. Depending on the conditions, the HCN released may react with the as yet unreacted hydride to produce H_2 and $[(^{13}CN)_4Pd]^{2-}$. Intuitively, the bulky, poorly coordinating organic cation should not influence the reactivity of HCN. In nonaqueous aprotic media, however, it apparently may do so, due to tight ion pairing (see below) that can involve specific interactions between the counterions. The Pd−CN ionization and sequential HCN reductive elimination should result in $[Pd(CN)]^-$ which decomposes to palladium metal and CN^-. Therefore, free cyanide is generated upon decomposition, which shifts the equilibrium between the unstable tricoordinate $[(CN)_2PdH]^-$ and stable tetracoordinate $[(CN)_3PdH]^{2-}$ toward the latter, thus decelerating and eventually terminating the decomposition process. The stability of the hydride and its lack of reactivity toward olefins in THF is accounted for by much more difficult Pd−CN ionization in the medium of considerably lower polarity. (b) Interestingly, when the reaction *under vacuum* was repeated in a flask that had not been flame-dried and using a teflon stopcock instead of flame sealing (i.e., under less rigorously anhydrous conditions), *both* $[(CN)_3PdBu]^{2-}$ and $[(CN)_3PdH]^{2-}$ were produced (see Experimental Section). This indicated that the $[(Ph_3P)_4Pd]/[Bu_4N]^+ CN^-$ system might be highly sensitive to microscopic quantities of water, as has now been established (see below).

(21) (a) All of the old Pd(0) reagent had been spent by the time the need emerged to analyze it for impurities. However, we customarily test the quality of any newly obtained $[(Ph_3P)_4Pd]$ reagents prior to use in our laboratories. This standard test includes reacting $[(Ph_3P)_4Pd]$ with PhI in benzene and analyzing the resulting solution by ^{31}P NMR. Integration of the singlets from the products, *trans*-$[(Ph_3P)_2Pd(Ph)I]$ (22.3 ppm, 1 equiv) and free PPh_3 (−5.5 ppm, 2 equiv) determines the composition of the Pd(0) compound in terms of the PPh_3 to palladium ratio. The amount of Ph_3PO impurity in the sample is easily estimated by integrating its ^{31}P NMR singlet (usually around 25−28 ppm) against those from $[(Ph_3P)_2Pd(Ph)I]$ and PPh_3. Judging by this test, both the old and new Pd(0) reagents were found to have the expected stoichiometry, $[(Ph_3P)_4Pd]$, and appeared to be pure, containing Ph_3PO in only trace amounts that were hardly ^{31}P NMR-detectable. (b) In the presence of water, the two reaction paths (eqs 2 and 3) compete, which results in the formation of *both* $[(CN)_3PdBu]^{2-}$ and $[(CN)_3PdH]^{2-}$. The $[(CN)_3PdBu]^{2-}$ to $[(CN)_3PdH]^{2-}$ product ratio was found to strongly decrease with an increase in the concentration of $[(Ph_3P)_4Pd]$. At $[[(Ph_3P)_4Pd]] > 0.08$ mol dm^{-3} with 1−5 equiv of H_2O per palladium, the reaction produces almost exclusively $[(CN)_3PdH]^{2-}$ and only barely observable amounts of $[(CN)_3PdBu]^{2-}$. This is in accord with the results of our kinetic studies of reaction 3 (see below), which show that the rate of formation of $[(CN)_3PdBu]^{2-}$ varies inversely with $[Pd(0)]$. Reaction 2 leading to the hydride $[(CN)_3PdH]^{2-}$ is not as dependent on $[(Ph_3P)_4Pd]$ concentration. (c) We cannot rule out the possibility of contamination of the old Pd(0) reagent with not only water but also some other impurities that, like H_2O, cannot be detected by the PhI test.[21a]

(22) Giannoccaro, P.; Sacco, A.; Vasapollo, G. *Inorg. Chim. Acta* **1979**, *37*, L455.

an unstable[18] phosphine palladium hydride, conceivably [(Ph$_3$P)$_2$-Pd(H)(^{13}CN)]. The latter would then react with another equiv of H^{13}CN to give rise to [(Ph$_3$P)$_2$Pd(^{13}CN)$_2$] and H$_2$, just as many [L$_n$Pd−H] complexes react with HX to give H$_2$ and [L$_n$-Pd−X].[18] Finally, the phosphine ligands on palladium would be easily displaced with excess cyanide,[9] resulting in stable tetracyanopalladate, the final product. Support for this proposal came from the detection of a hydrido palladium intermediate that was formed immediately upon treating a THF-d_8 solution of [(Ph$_3$P)$_4$Pd] with a ca. 2-fold excess of aqueous H^{13}CN. This species displayed a signal in the hydride region of the ^{1}H NMR spectrum (−8.7 ppm, d, J_{H-C} = 56.2 Hz) and was also detected by ^{13}C NMR (141.5 ppm, a singlet; a doublet with J_{H-C} = 56.2 Hz with the proton decoupler off). Other ^{1}H and ^{13}C NMR data were consistent with the presence of H^{13}CN[23] and H$_2$ (4.5 ppm, s).[24] As the reaction occurred, well-shaped colorless crystals formed, which were identified as *trans*-[(Ph$_3$P)$_2$Pd(CN)$_2$] by NMR and X-ray analysis.[25]

We also considered the reaction of K^{13}CN with [(Ph$_3$P)$_4$Pd] and H^{13}CN in the presence of 18-crown-6 in THF. The main product was again [(^{13}CN)$_4$Pd]$^{2-}$ (^{13}C NMR); however, the formation of ([K·18-crown-6]$^+$)$_2$ [(^{13}CN)$_3$PdH]$^{2-}$ in ca. 20−30% yield was also seen. The balance between the formation of [(CN)$_4$Pd]$^{2-}$ and [(CN)$_3$PdH]$^{2-}$ is clearly dependent on the nature of the cation, because with [Bu$_4$N]$^+$ ^{13}CN$^-$ the clean production of [(CN)$_3$PdH]$^{2-}$ was observed (see above). The formation of both species could involve an initial HCN oxidative addition to [(Ph$_3$P)$_4$Pd] to produce a phosphine Pd(II) cyano hydride [(Ph$_3$P)$_n$Pd(H)(CN)]. The latter could then undergo PPh$_3$ displacement with cyanide,[9] leading to [(CN)$_3$PdH]$^{2-}$. This path was favored for the [Bu$_4$N]$^+$ CN$^-$ reagent, a highly reactive source of cyanide with a weakly coordinating counterion. However, when KCN·18-crown-6 was used, the reactivity of cyanide was diminished due to its interactions with the potassium cation. As a result, PPh$_3$/CN$^-$ exchange leading to [(CN)$_3$PdH]$^{2-}$ was slower and the HCN that was still present could successfully compete for the reaction with the [(Ph$_3$P)$_n$Pd(H)(CN)] species to give H$_2$ and [(CN)$_4$Pd]$^{2-}$, as shown in eq 5.

Kinetic Studies on the Formation of [(CN)$_3$PdBu]$^{2-}$. To gain insight into the unusual C−N activation reaction leading to the formation of [(^{13}CN)$_3$PdBu]$^{2-}$ (eq 3), the kinetics of this process was studied by ^{13}C NMR using the new [(Ph$_3$P)$_4$Pd] reagent and [Bu$_4$N]$^+$ ^{13}CN$^-$. Details of these runs are presented in the Experimental Section. The reaction was >95% selective toward the formation of [(^{13}CN)$_3$PdBu]$^{2-}$ and exhibited first-order kinetics, as clearly indicated by the linearity of the logarithmic plots for product formation (Figure 6).

In the first series of experiments (Table 1), it was established that for the same concentration of [(Ph$_3$P)$_4$Pd] (1.7 × 10^{-2} mol dm^{-3}) reaction rates varied insignificantly upon changing the molar ratio of [Bu$_4$N]$^+$ ^{13}CN$^-$ to [(Ph$_3$P)$_4$Pd] from 4 to 3 and
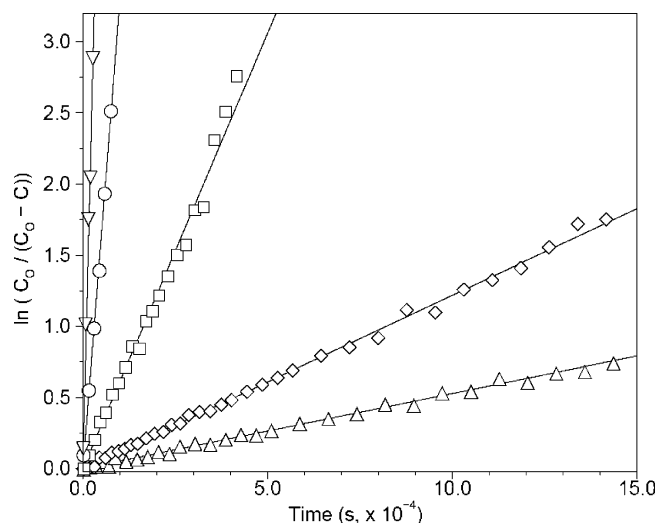
Figure 6. First-order kinetic plot for the formation of [(^{13}CN)$_3$PdBu]$^{2-}$ at 5 °C (△), 10 °C (◇), 20 °C (□), 30 °C (○), and 40 °C (▽) in THF-d_8. Data acquisition at 5 °C was continued out to 65.6 h.

then to 8 (entries 1−3).[26] In fact, slightly slower rates were observed at higher concentrations of the cyanide salt. To determine if the tetrabutylammonium cation and the cyanide anion, both involved in the reaction, had counterdirecting effects on rate, kinetic run 3 was repeated with half of the concentration of cyanide but with the same concentration of [Bu$_4$N]$^+$ (entry 4). The similar rate constants in these two experiments provided a clear indication of no counterdirecting effects involved and, overall, the rate of the reaction appears to be relatively unaffected by changes in [Bu$_4$N]$^+$ ^{13}CN$^-$ concentration. In contrast, lowering the concentration of [(Ph$_3$P)$_4$Pd] by a factor of 2 resulted in approximately twice as fast a reaction, regardless of the reagent ratio (entries 1, 5, and 6). Using [(Ph$_3$P)$_3$Pd] in place of [(Ph$_3$P)$_4$Pd] led to a slightly faster rate. It is well-known that in solution [(Ph$_3$P)$_4$Pd] is ca. 100% dissociated to [(Ph$_3$P)$_3$-Pd] and PPh$_3$ and that these species are involved in fast exchange at ambient temperature.[27] Larger quantities of extra phosphine inhibited the reaction more noticeably. For instance, in a separate semiquantitative experiment it was found that adding 6 equiv of PPh$_3$ decelerated the reaction of [(Ph$_3$P)$_4$Pd] under the standard conditions (Table 1, entry 1) by a factor of ca. 4.

Studying the kinetics of the formation of [(^{13}CN)$_3$PdBu]$^{2-}$ in the temperature range from 5 to 40 °C (Figure 6) allowed for the determination of the activation parameters of the reaction. The activation enthalpy and entropy were determined by direct nonlinear least-squares fitting of these parameters to the Eyring equation k_1 = (k_BT/h) exp($\Delta S^{\ddagger}/R$) exp($-\Delta H^{\ddagger}/RT$) using the temperature and rate constant data in Table 2. This gave the parameter estimates (25 °C) $\Delta G^{\ddagger}$ = 22.7 ± 0.1 kcal mol^{-1}, $\Delta H^{\ddagger}$ = 26.3 ± 0.7 kcal mol^{-1}, $\Delta S^{\ddagger}$ = 12 ± 2 cal mol^{-1} deg^{-1}, and E_a = 26.9 ± 0.7 kcal mol^{-1}.

The kinetic isotope effect (KIE) associated with the C−N activation was studied by reacting [(Ph$_3$P)$_4$Pd] with [(C$_4$D$_9$)$_4$N]$^+$ ^{13}CN$^-$ or [(CH$_3$CH$_2$CD$_2$CH$_2$)$_4$N]$^+$ ^{13}CN$^-$ (Table 3 and Figure S2 in the Supporting Information). For the fully deuterated cation, a modest KIE of k_H/k_D = 1.6 was measured at 20 °C. An even lower value of 1.3 was measured when [(CH$_3$CH$_2$CD$_2$-CH$_2$)$_4$N]$^+$ ^{13}CN$^-$ was used for the reaction.

(23) For the literature NMR data for H^{13}CN, see: Olah, G. A.; Kiovsky, T. E. *J. Am. Chem. Soc.* **1968**, *90*, 4666.
(24) Only one broad singlet (14.5 ppm, $\Delta\nu_{1/2}$ = 150 Hz) was observed in the ^{31}P NMR spectrum. This signal is believed to be from *trans*-[(Ph$_3$P)$_2$Pd-(H)(CN)] in fast exchange with free PPh$_3$. Analogous hydrido cyano nickel complexes stabilized by tertiary phosphines and phosphites have been shown to undergo such exchange that is fast on the NMR time scale, causing removal of H-P coupling: Druliner, J. D.; English, A. D.; Jesson, J. P.; Meakin, P.; Tolman, C. A. *J. Am. Chem. Soc.* **1976**, *98*, 2156.
(25) A crystal structure of *trans*-[(Ph$_3$P)$_2$Pd(CN)$_2$]·CH$_2$Cl$_2$ has been reported: Hua, R.; Gota, M.; Tanaka, M. *Anal. Sci.* **2001**, *17*, 469.

(26) The lowest [Bu$_4$N]$^+$ ^{13}CN$^-$ to [(Ph$_3$P)$_4$Pd] molar ratio of 3 used in the kinetic runs was dictated by the stoichiometry of the reaction (eq 3).
(27) Mann, B. E.; Musco, A. *J. Chem. Soc., Dalton Trans.* **1975**, 1673.

Table 1. Kinetic Data for Reaction 3 in THF-d_8 at 20 °C

entry	Pd(0) complex	[Pd], mol dm^{-3}	[Bu$_4$N$^+$ ^{13}CN$^-$], mol dm^{-3}	additive (concentration)	$k \times 10^5$, s^{-1}
1	[(Ph$_3$P)$_4$Pd]	1.7×10^{-2}	7.0×10^{-2}		5.95 ± 0.19
2	[(Ph$_3$P)$_4$Pd]	1.7×10^{-2}	5.2×10^{-2}		6.49 ± 0.19
3	[(Ph$_3$P)$_4$Pd]	1.7×10^{-2}	14.0×10^{-2}		4.65 ± 0.20
4	[(Ph$_3$P)$_4$Pd]	1.7×10^{-2}	7.0×10^{-2}	[Bu$_4$N]$^+$ BF$_4^-$ (7.0×10^{-2} mol dm^{-3})	4.01 ± 0.11
5	[(Ph$_3$P)$_4$Pd]	0.8×10^{-2}	7.0×10^{-2}		10.94 ± 0.24
6	[(Ph$_3$P)$_4$Pd]	0.8×10^{-2}	3.5×10^{-2}		9.24 ± 0.22
7	[(Ph$_3$P)$_3$Pd]	1.7×10^{-2}	7.0×10^{-2}		6.65 ± 0.16

Table 2. VT Kinetic Data for Reaction 3 in THF-d_8 at [(Ph$_3$P)$_4$Pd] = 1.7×10^{-2} mol dm^{-3}

temp, °C	k, s^{-1}
5	$5.34 \pm 0.23 \times 10^{-6}$
10	$1.21 \pm 0.04 \times 10^{-5}$
20	$5.95 \pm 0.19 \times 10^{-5}$
30	$2.97 \pm 0.08 \times 10^{-4}$
40	$1.19 \pm 0.07 \times 10^{-3}$

Table 3. KIE for Reaction 3 ([(Ph$_3$P)$_4$Pd] = 1.7×10^{-2} mol dm^{-3}) in THF-d_8 at 20 °C

cyanide source (7.0×10^{-2} mol dm^{-3})	$k \times 10^5$, s^{-1}
[Bu$_4$N]$^+$ ^{13}CN$^-$	5.95 ± 0.19
[(C$_4$D$_9$)$_4$N]$^+$ ^{13}CN$^-$	3.52 ± 0.10
[(CH$_3$CH$_2$CD$_2$CH$_2$)$_4$N]$^+$ ^{13}CN$^-$	4.39 ± 0.12

The presence of a KIE was confirmed by independent semiquantitative experiments. A solution of [(Ph$_3$P)$_4$Pd] in THF-d_8 was divided into two equal parts, of which one was reacted with 4 equiv of [Bu$_4$N]$^+$ ^{13}CN$^-$ and the other with 4 equiv of [(C$_4$D$_9$)$_4$N]$^+$ ^{13}CN$^-$. At room temperature, it took the reaction involving the deuterated cation about twice as long to go to completion, as was judged by full color loss and confirmed by ^{13}C NMR. Analysis of the two reaction solutions by ^{13}C NMR revealed that the signals from the cyano ligand on palladium trans to n-C$_4$H$_9$ and n-C$_4$D$_9$ were sufficiently separated for integration. This led to another experiment, in which 1 equiv of [(Ph$_3$P)$_4$Pd] was reacted with a solution of 10 equiv of [Bu$_4$N]$^+$ ^{13}CN$^-$ and 10 equiv of [(C$_4$D$_9$)$_4$N]$^+$ ^{13}CN$^-$. After this reaction had gone to completion, the KIE was estimated at ca. 2 by integrating the triplet resonances from the [(^{13}CN)$_3$Pd-(C$_4$H$_9$)]$^{2-}$ and [(^{13}CN)$_3$Pd(C$_4$D$_9$)]$^{2-}$, as shown in Figure S3 in the Supporting Information. This experiment ruled out the possibility that the difference in reaction rates observed in the other experiments was due to some impurities in the samples of [Bu$_4$N]$^+$ ^{13}CN$^-$ and [(C$_4$D$_9$)$_4$N]$^+$ ^{13}CN$^-$, rather than the actual KIE.

Low-Temperature ^{13}C and ^{31}P NMR Studies of the [(Ph$_3$P)$_4$Pd]/[Bu$_4$N]$^+$ ^{13}CN$^-$ System. To gain insight into the nature of the reactive Pd(0) species that are formed upon mixing [(Ph$_3$P)$_4$Pd] and [Bu$_4$N]$^+$ ^{13}CN$^-$ in THF, we attempted their characterization. Unfortunately, despite repeated attempts we were unable to isolate any of these mixed cyano-phosphine Pd-(0) complexes for an X-ray study, although in the course of this work an unusual dioxygen adduct, [K·18-crown-6]$^+$ [(Ph$_3$P)Pd(CN)(O$_2$)]$^-$, was characterized crystallographically (Figure 7).[28] Therefore, the [(Ph$_3$P)$_4$Pd]/[Bu$_4$N]$^+$ ^{13}CN$^-$ system was studied by low-temperature ^{13}C and ^{31}P NMR. The two reagents in a 1:4.7 palladium to CN ratio were dissolved in a mixture of THF and THF-d_8 at -78 °C, and the resulting solid-free, tan-yellow solution was immediately placed in an NMR
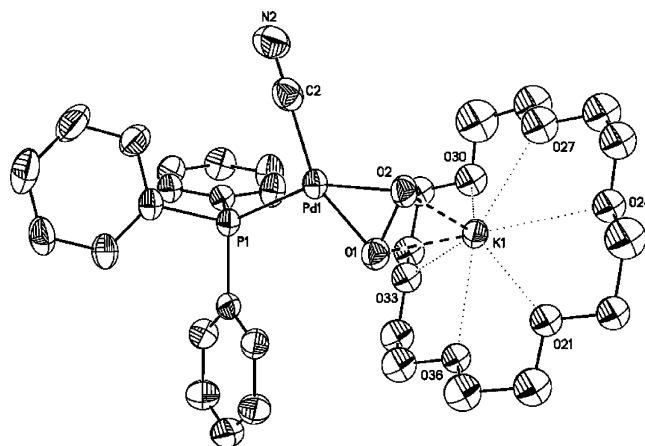
Figure 7. ORTEP drawing of [K·18-crown-6]$^+$ [(Ph$_3$P)Pd(CN)(O$_2$)]$^-$ with thermal ellipsoids drawn to the 50% probability level. Selected bond distances (Å) and bond angles (deg): Pd(1)−C(2) 1.981(6), Pd(1)−O(1) 1.990(3), Pd(1)−O(2) 2.016(3), Pd(1)−P(1) 2.253(1), O(2)−O(1) 1.441-(4), O(2)−K(1) 2.697(3), O(1)−K(1) 2.784(3), C(2)−Pd(1)−O(1) 154.6-(2), C(2)−Pd(1)−O(2) 112.5(2), O(1)−Pd(1)−O(2) 42.2(1), C(2)−Pd(1)−P(1) 93.5(1), O(1)−Pd(1)−P(1) 111.9(1), O(2)−Pd(1)−P(1) 154.0(1), N(2)−C(2)−Pd(1) 177.4(5).

probe at -80 °C. The spectra were acquired with sufficient delay to ensure integration accuracy. Both ^{13}C and ^{31}P NMR spectra were recorded in the sequence -80, -60, 0, and -20 °C. The

(28) Preparing concentrated solutions of [(Ph$_3$P)$_4$Pd] and [Bu$_4$N]$^+$ CN$^-$ in THF at 0 °C and then cooling them to -25 °C and below commonly resulted in precipitation of yellow crystals, which, unfortunately, were never of X-ray quality. The choice of cations and solvents for the reaction of [(Ph$_3$P)$_4$Pd] with cyanide is very limited. For instance, [Et$_4$N]$^+$ CN$^-$ is insoluble in THF but soluble in MeCN, whereas [(Ph$_3$P)$_n$Pd] (n = 3, 4) is soluble in THF but insoluble in acetonitrile. Although KCN is poorly soluble in THF in the presence of 18-crown-6, it was found to dissolve readily upon addition of [(Ph$_3$P)$_4$Pd]. After THF solutions containing [(Ph$_3$P)$_4$Pd], KCN, and 18-crown-6 in a 1:2:2 ratio had been prepared at room temperature and then kept at -25 °C overnight or slowly evaporated, yellow plates of [(Ph$_3$P)$_4$-Pd]·THF (X-ray) and tiny white needles of [KCN·18-crown-6] precipitated out. The crystallization process was obviously driven by the poor solubility of [KCN·18-crown-6] rather than by any enhanced stability of mixed phosphine cyanide anions at lower temperatures. Upon collection of one of the yellow plates of [(Ph$_3$P)$_4$Pd]·THF for X-ray analysis, the entire mixture was exposed to air. Six hours later, the appearance of some new, faint amber needle-shaped crystals was noticed. One of those was studied by X-ray diffraction to reveal an interesting structure of a palladium complex containing one PPh$_3$, one CN$^-$, and one O$_2$ molecule bound to the metal (Figure 7). Both oxygen atoms also form contacts to the potassium cation inside the crown. The O−O bond distance of 1.441(4) Å is within the range of 1.37−1.48 Å observed for other structurally characterized dioxygen complexes of palladium: Yoshida, T.; Tatsumi, K.; Matsumoto, M.; Nakatsu, K.; Nakamura, A.; Fueno, O.; Otsuka, S. *New J. Chem.* **1979**, *3*, 761. Stahl, S. S.; Thorman, J. L.; Nelson, R. C.; Kozee, M. A. *J. Am. Chem. Soc.* **2001**, *123*, 7188. Clegg, W.; Eastham, G. R.; Elsegood, M. R. J.; Heaton, B. T.; Iggo, J. A.; Tooze, R. P.; Whyman, R.; Zacchini, S. *J. Chem. Soc., Dalton Trans.* **2002**, 3300. Miyaji, T.; Kujime, M.; Hikichi, S.; Moro-oka, Y.; Akita, M. *Inorg. Chem.* **2002**, *41*, 5286. Aboelella, N. W.; York, J. T.; Reynolds, A. M.; Fujita, K.; Kinsinger, C. R.; Cramer, C. J.; Riordan, C. G.; Tolman, W. B. *Chem. Commun.* **2004**, 1716. Konnick, M. M.; Guzei, I. A.; Stahl, S. S. *J. Am. Chem. Soc.* **2004**, *126*, 10212. Adjabeng, G.; Brenstrum, T.; Frampton, C. S.; Robertson, A. J.; Hillhouse, J.; McNulty, J.; Capretta, A. *J. Org. Chem.* **2004**, *69*, 5082. Yamashita, M.; Goto, K.; Kawashima, T. *J. Am. Chem. Soc.* **2005**, *127*, 7294.

Table 4. Variable Temperature ^{31}P and ^{13}C NMR Data for a Solution of $[(Ph_3P)_4Pd]$ (6.7×10^{-3} mol dm^{-3}) and $[Bu_4N]^+$ $^{13}CN^-$ (31.6×10^{-3} mol dm^{-3}) in THF/THF-d_8 (3:1)^a

		equiv per Pd (^{31}P NMR)		equiv per Pd (^{13}C NMR)	
entry	T, °C	free PPh$_3$ (−5 ppm)	bound PPh$_3$ (21 ppm)	free CN$^-$ (167 ppm)	bound CN$^-$ (ca. 159 ppm)
1	−80	1.4	2.6	4	0.7
2	−60	1.7	2.3	4	0.7
3	0	4.0 (coalescence)		3.9	0.8
4	−20^b	2.7	1.3	3.9	0.8
5	−40	2.4	1.6	4.1	0.6
6	−60	2.0	2.0	4.1	0.6

^{a} The molar ratio of Pd/PPh$_3$/CN$^-$ = 1:4:4.7 (see text). ^{b} Kept at −20 °C for 48 h prior to further studies (entries 4−6).

sample was then stored at −20 °C for 48 h, after which time the study was resumed to obtain the data at −40 °C and then again at −60 °C. No C−P coupling was observed throughout the experiment in the temperature range of 0 to −80 °C.[29] The lack of multiplicity for the observed signals was most unfortunate because it strongly impeded unambiguous interpretation of the composition and structure of the mixed phosphine cyanide Pd(0) species. Nonetheless, some conclusions could be drawn from the integration data for the free and coordinated PPh$_3$ and $^{13}CN^-$ (Table 4).

As can be seen from Table 4, of the total of 4.7 equiv of cyanide per palladium present in the system, approximately one remained coordinated to the metal, regardless of the temperature. At least two Pd−CN species could be observed, as judged by the appearance of two signals around 159 ppm in the ^{13}C NMR spectra. While the linewidths, exact chemical shifts, and relative intensities of the two resonances varied at different temperatures, the two together consistently integrated against the singlet from the free cyanide (167 ppm) as 0.6−0.8 to 3.9−4.1. In contrast, the coordinated PPh$_3$ (21 ppm) to free PPh$_3$ (−5 ppm) ratio varied throughout the experiment. The degree of PPh$_3$ binding was different at −60 °C after this temperature was approached from ca. −80 °C an hour or so after the sample was prepared, and later on, after the sample had been warmed to 0 °C, kept at −20 °C for 2 days, and finally cooled back. Apparently, exposure of the sample to higher temperatures led to more efficient phosphine loss from the metal. The free to coordinated phosphine ratio of 1:1 observed at −60 °C toward the end of the experiment is indicative that, on average, only two PPh$_3$ ligands were bound to palladium at that point, along with one cyanide. Importantly, even *less than two* PPh$_3$ molecules per palladium appeared to be coordinated at −20 and −40 °C (entries 4 and 5 in Table 4).

The VT NMR studies indicated that a solution of $[(Ph_3P)_4Pd]$ and $[Bu_4N]^+$ CN$^-$ in THF is a complex system that involves temperature-dependent and not necessarily fast equilibria between various mixed phosphine cyanide Pd(0) species. While stoichiometry considerations along with the VT NMR data (Table 4) suggest that $[(Ph_3P)_2Pd(CN)]^-$ is likely to be the main species present when the system is roughly equilibrated at −60 °C, care should be exercised when proposing structures of the actual complexes in the solution. Like conventional quaternary ammonium salts in media of low polarity,[30] ionic phosphine cyanide Pd(0) species are expected to exist in THF

as aggregates of tight ion pairs. The lack of observable ^{31}P−^{13}C coupling in the NMR spectra limited significantly the amount of structural information that could be extracted from these experiments.

Computational Studies

C−N Bond Activation in the $[(Ph_3P)_4Pd]/[Bu_4N]^+$ CN$^-$ System under Anhydrous Conditions. Density functional theory (DFT) calculations have been carried out to assess possible mechanisms for the C−N bond activation reaction exhibited by the $[(Ph_3P)_4Pd]/[Bu_4N]^+CN^-$ system. In the majority of our calculations, $[Bu_4N]^+$ has been simplified to $[Me_3NEt]^+$, whereas PPh$_3$ is replaced with PH$_3$. A number of test calculations with PPh$_3$ and various larger $[R_4N]^+$ cations have also been performed to assess the role of steric bulk (see below). Two general processes for the reaction of the $[R_4N]^+$ species with a metal fragment, L$_n$M, have been considered, namely, (a) Hofmann elimination or (b) oxidative addition (Scheme 3). Within these two classes, Hofmann elimination may occur in either an anti or syn fashion, while oxidative addition may proceed via a concerted 3-membered process or an S$_N$2-type displacement of amine. Note that oxidative addition yields the observed metal−alkyl product directly, whereas Hofmann elimination links to a metal hydride. In principle, the alkyl product could then be produced by this latter route via subsequent alkene migratory insertion.
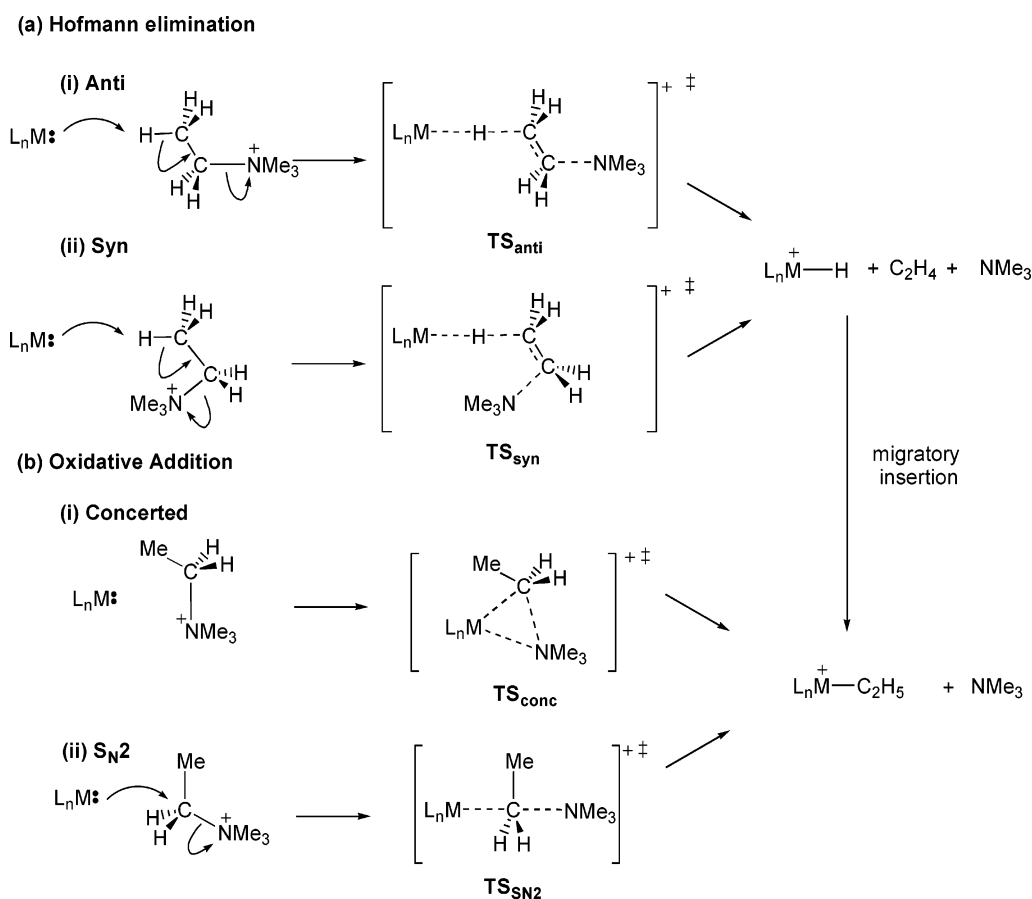
2-Coordinate Models. The initial choice of the model for the reactive metal fragment, L$_n$M, is based on the data in Table 4, which indicate $[(PPh_3)_2Pd(CN)]^-$ to be the dominant species at −60 °C but that warming facilitates further PPh$_3$ dissociation. Our initial focus will therefore be on the 2-coordinate $[(PH_3)Pd(CN)]^-$ model species. A 3-coordinate complex acting as the *active* species cannot be ruled out, however, especially given the role proposed for such species in the oxidative addition of aryl halides.[31−33] A second set of calculations was therefore carried out with $[(PH_3)_2Pd(CN)]^-$. One further issue is that in THF anionic palladium-cyano species would be expected to form ion pairs and aggregates with $[NR_4]^+$ cations.[30] To reflect this, our starting model reactant in the $[(PH_3)Pd(CN)]^-/[Me_3NEt]^+$ system will be the ion pair, **1**, the computed structure of which is shown in Figure 8.

Within **1**, the individual ions show their expected linear and tetrahedral geometries, although a slight bending of the $[(PH_3)Pd(CN)]^-$ moiety at palladium and C1 is computed (P−Pd−C1 = 176.7°, Pd−C1−N1 = 172.4°). This presumably arises from the attractive electrostatic interaction between the two species and indeed N1, in particular, is computed to carry a significant negative charge (−0.46) that attracts the δ^+ methyl

(29) Cooling the sample to −90 and further to −100 °C resulted in broader lines, apparently due to higher viscosity.

(30) See, for example: (a) Ivashkevich, A. N.; Kostynyuk, V. P. *Zh. Fiz. Khim.* **1991**, *65*, 948 and references cited therein. (b) Everaert, J.; Persoons, A. *J. Phys. Chem.* **1981**, *85*, 3930. (c) Barker, C.; Yarwood, J. *Faraday Symp. Chem. Soc.* **1977**, 136. (d) Mo, H.; Wang, A.; Wilkinson, P. S.; Pochapsky, T. C. *J. Am. Chem. Soc.* **1997**, *119*, 11666.

(31) For selected original reports, see: (a) Amatore, C.; Jutand, A.; Suarez, A. *J. Am. Chem. Soc.* **1993**, *115*, 9531. (b) Jutand, A.; Mosleh, A. *Organometallics* **1995**, *14*, 1810. (c) Amatore, C.; Carre, E.; Jutand, A.; M'Barki, M. A. *Organometallics* **1995**, *14*, 1818. (d) Amatore, C.; Carre, E.; Jutand, A.; M'Barki, M. A.; Meyer, G. *Organometallics* **1995**, *14*, 5605.

(32) For reviews, see: Amatore, C.; Jutand, A. *J. Organomet. Chem.* **1999**, *576*, 254. Amatore, C.; Jutand, A. *Acc. Chem. Res.* **2000**, *33*, 314.

(33) For computational studies, see: (a) Kozuch, S.; Shaik, S.; Jutand, A.; Amatore, C. *Chem.−Eur. J.* **2004**, *10*, 3072. (b) Amatore, C.; Jutand, A.; Lemaitre, F.; Ricard, J. L.; Kozuch, S.; Shaik, S. *J. Organomet. Chem.* **2004**, *689*, 3728. (c) Kozuch, S.; Amatore, C.; Jutand, A.; Shaik, S. *Organometallics*, **2005**, *24*, 2319.

Scheme 3

(a) Hofmann elimination

(i) Anti

TS_{anti}

(ii) Syn

TS_{syn}

$$L_nM\overset{+}{\longrightarrow}H \;+\; C_2H_4 \;+\; NMe_3$$

migratory
insertion

(b) Oxidative Addition

(i) Concerted

TS_{conc}

$$L_n\overset{+}{M}\!\!-\!C_2H_5 \quad + \quad NMe_3$$

(ii) S_N2

TS_{SN2}

hydrogens and results in a number of short inter-ion contacts.[34] Both of these effects are slightly exaggerated in the gas-phase geometry, and solution-phase optimization leads to a somewhat looser structure where the shortest inter-ion contact is 2.29 Å (N1···H3) and the [(PH$_3$)Pd(CN)]$^-$ moiety is closer to linear (P−Pd−C1 = 178.7°, Pd−C1−N1 = 177.3°). Similar structural changes are also seen when comparing gas-phase and solution-phase optimized geometries for other species in this study (see Experimental Section).

The four transition states for C−N activation derived from **1** are shown in Figure 9. In the Hofmann elimination reactions via **TS1$_{anti}$** and **TS1$_{syn}$** concerted C−N and C−H bond activation occur, and in both cases rather late transition-state structures are computed with short Pd···H1 distances below 1.65 Å, elongated N1···C3 distances, and a shortening of the C2−C3

bond that indicates the onset of double-bond character in the putative alkene moiety. The anti and syn processes entail barriers of around 24 kcal/mol in the gas phase, which increase to 30 kcal/mol upon solvent correction. The increased barriers computed in THF reflect the reduced dipoles of **TS1$_{anti}$** and **TS1$_{syn}$** compared to ion pair **1**, and as a result the PCM stabilization is greater for the reactant than for the transition states. The reduction in the dipole arises from a more even charge distribution in the transition states. In particular, for **TS1$_{anti}$** and **TS1$_{syn}$** the incipient protonation of the metal center markedly lowers the negative charge on palladium from −0.46 in **1** to around 0 in the transition states. Similar effects account for the increased barriers computed in solution via **TS1$_{SN2}$** and **TS1$_{conc}$** below.

For the oxidative addition processes, concerted C−N activation via **TS1$_{conc}$** is computed to entail a prohibitively high barrier of almost 34 kcal/mol in the gas phase, which increases to 38.4 kcal/mol upon solvent correction. The latter value can be compared with a computed barrier of 18.6 kcal/mol for C−N activation in an allyl−ammonium cation by [(PH$_3$)$_2$Ni].[13g] The substantially lower barrier in the nickel case may arise from precoordination of the allylic double bond, which facilitates C−N cleavage. Certainly, without this feature concerted activation appears to be untenable, and the very long distances between the Pd, C3, and N2 reactive centers in **TS1$_{conc}$** are suggestive of excessive steric strain in this structure.

1
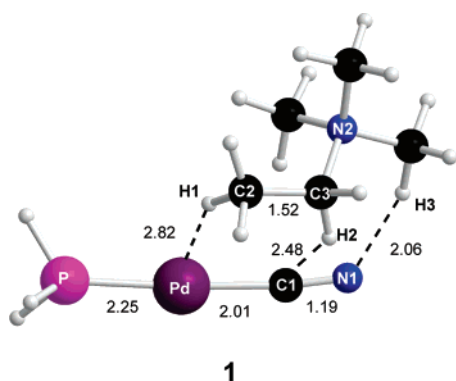
**Figure 8.** Computed reactant ion pair [(PH$_3$)Pd(CN)]$^-$·[Me$_3$NEt]$^+$ (**1**) with selected distances in Å.

(34) During the course of our studies, a number of alternative structures for **1** were located which feature different orientations of [Me$_3$NEt]$^+$ relative to [Pd(CN)(PH$_3$)]$^-$. Of these, **1** is the most stable, although the alternative structures are all within 1.5 kcal/mol.
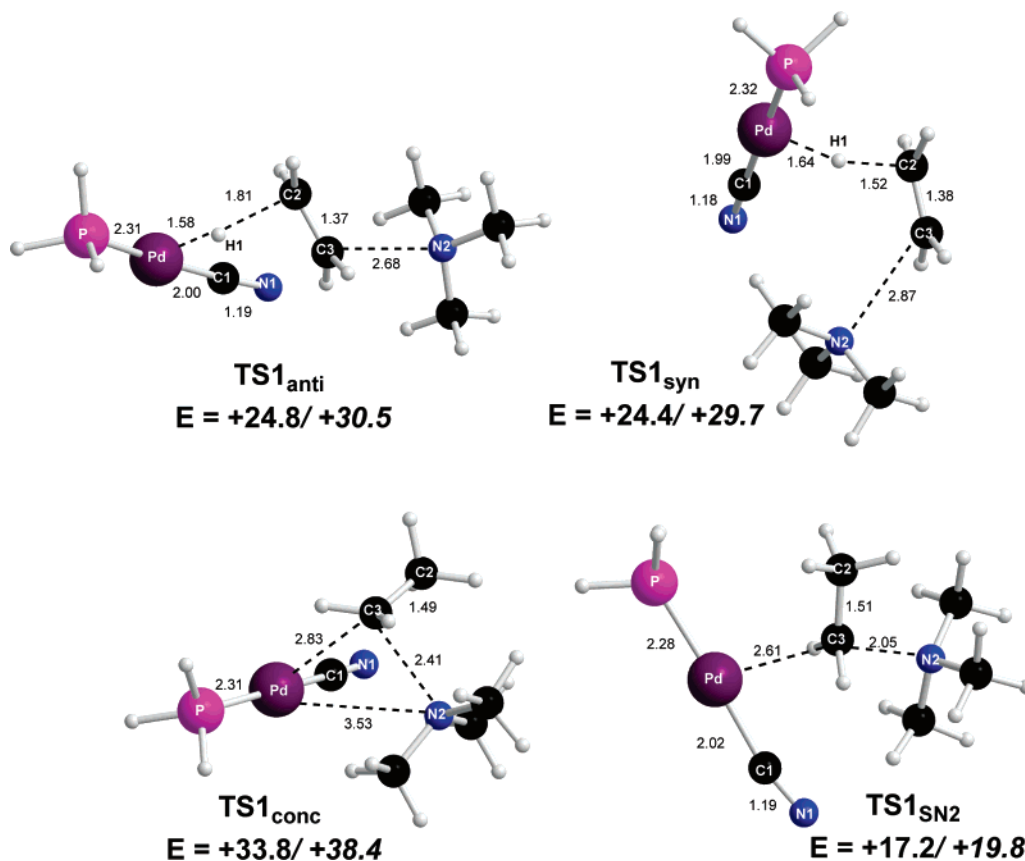
Figure 9. Computed transition state geometries for C−N activation in the [(PH$_3$)Pd(CN)]$^-$·[Me$_3$NEt]$^+$ ion pair (**1**) with selected distances in Å. Energies (kcal/mol) are given relative to **1** for the gas phase (plain text) and in THF solution (italics).
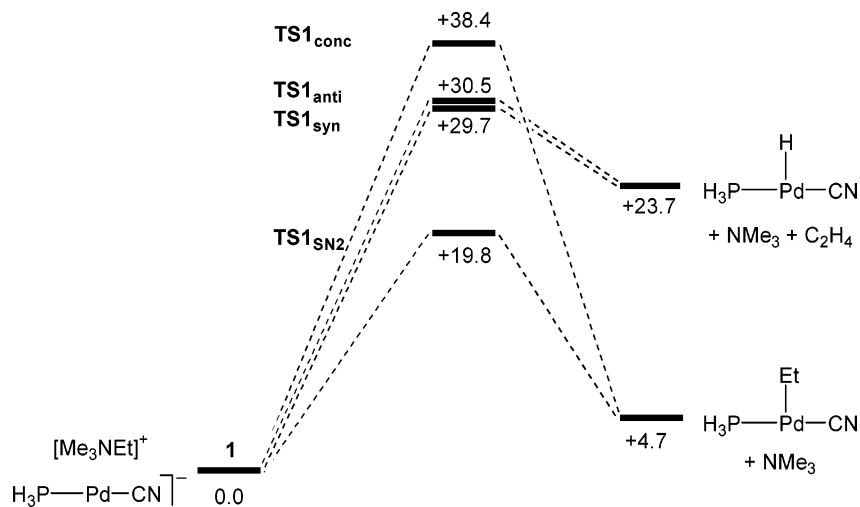

Figure 10. Computed solvent-corrected reaction profiles (kcal/mol) for C−N activation in **1**.

In contrast, in the S$_N$2 oxidative addition process [(PH$_3$)-Pd(CN)]$^-$ can attack from the less hindered face of the ethyl moiety and the resultant transition state, **TS1$_{SN2}$**, is much more accessible ($E = +17.2$ kcal/mol in the gas phase, rising to $+19.8$ kcal/mol in solution). **TS1$_{SN2}$** exhibits a classical trigonal bipyramidal geometry at C3, with the C3−N2 bond lengthening to 2.05 Å, while the Pd···C3 distance is 2.61 Å. These values suggest a relatively early transition state, and this notion is in line with the S$_N$2 mechanism being clearly the most kinetically accessible process of all of those considered from **1,** as summarized in Figure 10. Figure 10 also emphasizes the far

greater stability of the 3-coordinate palladium−alkyl species formed via oxidative addition over the alternative palladium−hydride formed via Hofmann elimination. The release of both NMe$_3$ and C$_2$H$_4$ makes this latter process more favored entropically. However, the computed free energies indicate that oxidative addition remains more stable ($\Delta G = -7.1$ kcal/mol cf. $\Delta G = +1.4$ kcal/mol for Hofmann elimination). The computed $\Delta G^\ddagger$ values are less affected and are all within 1.7 kcal/mol of the enthalpies reported in Figure 10.

3-Coordinate Models. The computed structure of the most stable form of the ion pair [(PH$_3$)$_2$Pd(CN)]$^-$·[Me$_3$NEt]$^+$, **2**, is

Scheme 4
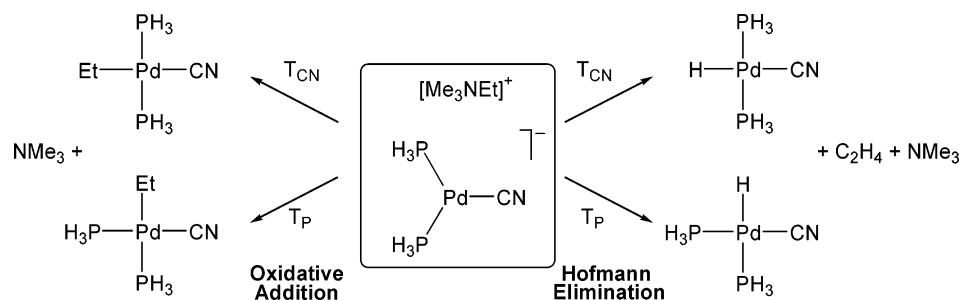
displayed in Figure 11 and shows the position of the $[Me_3NEt]^+$ cation relative to the CN^- ligand to be very similar to that described above in **1**. C–N activation in **2** will lead directly to 4-coordinate products in which the new hydride or alkyl ligand may be trans to either PH_3 or CN^- (T_P and T_{CN}, respectively, Scheme 4). There are therefore, in principle, a total of eight possible reaction pathways stemming from ion pair **2**.

For the T_P pathways, all four possible C–N activation reactions have been fully characterized, and the trends that emerge are very similar to those found previously with the 2-coordinate model. Thus, the most accessible process involves the S_N2 attack of palladium at C3 and this proceeds via $\mathbf{TS2_{SN2}}$ ($\mathbf{T_P}$) with a gas-phase activation energy of +17.8 kcal/mol or +23.6 kcal/mol in solution (Figure 12). The structure of $\mathbf{TS2_{SN2}}$ ($\mathbf{T_P}$) shows that the $\{P_2Pd(CN)\}$ core distorts to a T-shaped geometry to accept the ethyl group trans to P2. This additional PH_3 stays bound during the C–N activation process (Pd–P2 = 2.43 Å). Otherwise, the structure is very similar to $\mathbf{TS1_{SN2}}$, although the key Pd···C3 and C3···N2 distances are slightly longer in the 3-coordinate model. Relative energies (with solvent-corrected values in italics) for the remaining transition states follow the trend $\mathbf{TS2_{anti}}$ ($\mathbf{T_P}$) (+21.7/*26.1* kcal/mol) < $\mathbf{TS2_{syn}}$ ($\mathbf{T_P}$) = (+23.3/*29.8* kcal/mol) < $\mathbf{TS2_{conc}}$ ($\mathbf{T_P}$) (+32.7/*39.1* kcal/mol). Full structural details for these processes are given in the Supporting Information.

For the T_{CN} processes, despite repeated efforts,[35] it has only proven possible to locate the S_N2 transition state, $\mathbf{TS2_{SN2}}$ ($\mathbf{T_{CN}}$) (Figure 12). The behavior of this species is rather different from the T_P transition states. For example, unlike $\mathbf{TS2_{SN2}}$ ($\mathbf{T_P}$) where an incipient square-planar geometry was seen, in $\mathbf{TS2_{SN2}}$ ($\mathbf{T_{CN}}$) the ethyl group is forced to approach from above the trigonal $\{P_2Pd(CN)\}$ unit. The resultant structure exhibits a 'D_{2d}' geometry (P1–Pd–P2 = 136.7°; C1–Pd–C3 = 134.3°) and also features an agostic interaction with the C2–H1 bond (Pd···H1 = 2.07 Å; C2–H1 = 1.14 Å). Moreover, $\mathbf{TS2_{SN2}}$ ($\mathbf{T_{CN}}$) is unique in being stabilized relative to the ion-pair reactant upon PCM solvent correction. This result reflects the computed dipole moments, p, of the various stationary points involved. For **2**, $p = 11.5$ D, a much higher value than any of

the T_P transition states ($p = 6–7$ D). The PCM stabilization is therefore greater for **2**, leading to the relative destabilization of the T_P structures. In contrast, for $\mathbf{TS2_{SN2}}$ ($\mathbf{T_{CN}}$) $p = 18.2$ D, and this leads to a greater PCM stabilization than for **2** and a relative stabilization of $\mathbf{TS2_{SN2}}$ ($\mathbf{T_{CN}}$) upon solvent correction. This different behavior of $\mathbf{TS2_{SN2}}$ ($\mathbf{T_{CN}}$) can also be related to its structure in which the CN^- ligand is much more exposed than in any of the other transition states as a result of the loss of the stabilizing electrostatic interactions with the $[Me_3NEt]^+$ cation. This 'desolvation' of the CN^- ligand accounts for the larger gas-phase activation barrier compared to that computed for $\mathbf{TS2_{SN2}}$ ($\mathbf{T_P}$). For the same reason, however, resolution of the exposed CN^- group through the PCM correction then produces an enhanced stabilization for $\mathbf{TS2_{SN2}}$ ($\mathbf{T_{CN}}$) and drops the energy of this species below that of $\mathbf{TS2_{SN2}}$ ($\mathbf{T_P}$). It is important to stress that this result does not reflect the strategy of correcting gas-phase optimized energies with a single-point PCM correction, as full optimization of both **2** and $\mathbf{TS2_{SN2}}$ ($\mathbf{T_{CN}}$) in THF solvent produced essentially the same activation barrier (see Experimental Section and the Supporting Information).

The three lowest-energy routes for C–N activation in **2** are summarized in Figure 13, which shows that both S_N2 processes entail lower barriers than the lowest Hofmann elimination pathway via $\mathbf{TS2_{anti}}$ ($\mathbf{T_P}$). Moreover, the 4-coordinate palladium–alkyl products are significantly more stable than the analogous palladium–hydrides. As in the reactions of **1**, entropy will tend to make the Hofmann elimination products more accessible than what is implied in Figure 13. However, the computed relative free energies of the products show that *cis-*
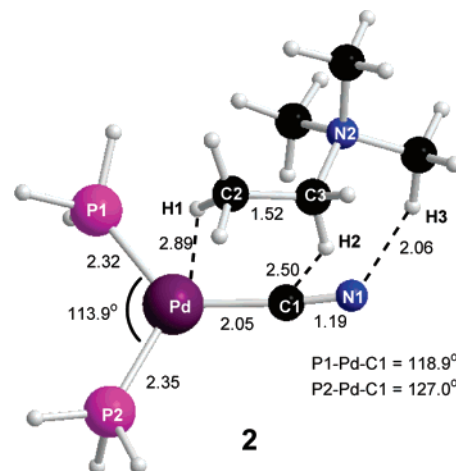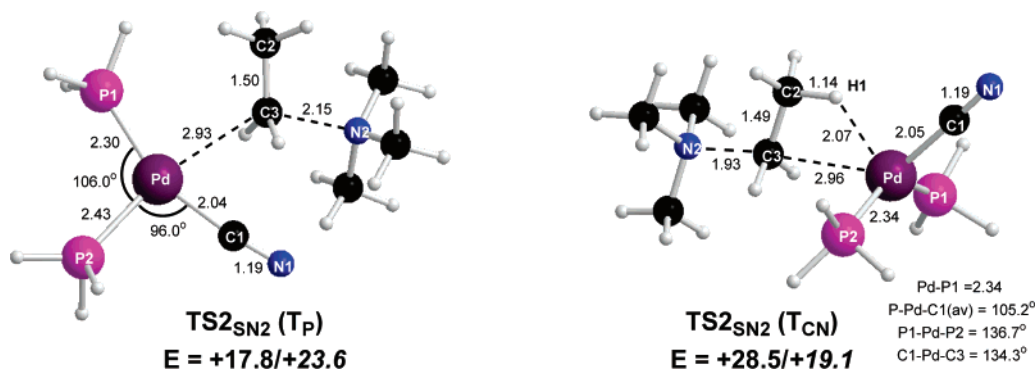
(35) Although linear transits for the other T_{CN} processes produced promising guess geometries, subsequent transition state optimizations failed, converging instead onto 2- or 3-coordinate product geometries or $\mathbf{TS_{SN2}}$ ($\mathbf{T_{CN}}$). This may reflect the intrinsic difficulty in distorting the $\{Pd(CN)P_2\}$ core: a T_{CN} $[Pd(CN)(PH_3)_2]^-$ geometry (i.e. with P1/P2–Pd–C1 fixed at 90°) lies 9.8 kcal/mol above optimized $[Pd(CN)(PH_3)_2]^-$, whereas the T_P form (P1–Pd–P2 = P1–Pd–C1 = 90°) is only 1.8 kcal/mol higher in energy. In addition, for Hofmann elimination the product, *trans-*$[Pd(CN)(PH_3)_2H]$, is relatively high in energy (+14.7 kcal/mol, see Figure 13) and, although this does not rule out this process, it does suggest that any transition state is unlikely to be lower in energy than $\mathbf{TS_{SN2}}$ ($\mathbf{T_{CN}}$). In addition, based on the trends computed for the reactions of **1** and **2** (via the T_P structures) we would expect the S_N2 mechanism to be the most accessible of the T_{CN} pathway.

Figure 11. Computed reactant ion pair $[(PH_3)_2Pd(CN)]^-\cdot[Me_3NEt]^+$ (**2**) with selected distances (Å) and angles.

Figure 12. Computed S$_{N}$2 transition states for C−N activation in [(PH$_3$)$_2$Pd(CN)]$^-$·[Me$_3$NEt]$^+$ (**2**) with selected distances (Å) and angles. Energies (kcal/mol) are given relative to **2** for the gas phase (plain text) and in THF solution (italics).
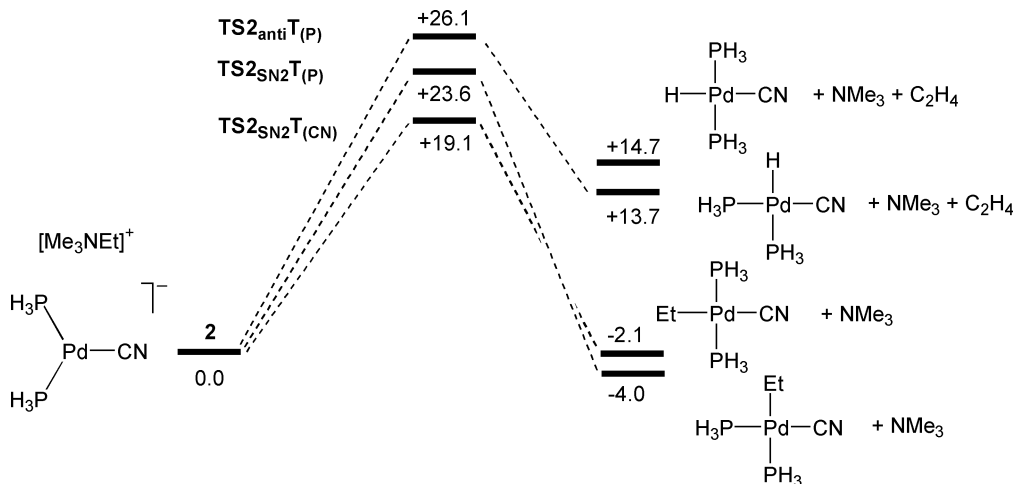
Figure 13. Computed solvent-corrected energy profiles (kcal/mol) for the lowest-energy C−N bond activation reactions of ion pair **2**. The energy of *trans*-[(PH$_3$)$_2$Pd(CN)H] is also included for comparison, although no direct pathway to this species could be located.

[(PH$_3$)$_2$Pd(CN)Et] is still the most accessible species (G = −14.4 kcal/mol compared to around −7 kcal/mol for *trans*-[(PH$_3$)$_2$Pd(CN)Et] and *cis/trans*-[(PH$_3$)$_2$Pd(CN)H]). Thus, essentially the same conclusion can be drawn from both the 2- and 3-coordinate models: C−N activation will occur via an S$_{N}$2 process to give directly a palladium−alkyl species, whereas the alternative Hofmann elimination/alkene insertion route is higher in energy. Interestingly, the lowest-energy processes from **1** and **2** both have activation barriers of ca. 19 kcal/mol in THF and so the identity of the active species cannot be distinguished on that basis. To probe this issue further, the energy for the formation of **2** from **1** was computed. This was found to be slightly exothermic (ΔE = −3.7 kcal/mol, solvent corrected), although the unfavorable loss of entropy makes the phosphine addition endergonic (ΔG = +5.8 kcal/mol). On this basis, ion-pair **1** containing a 2-coordinate {(PR$_3$)Pd(CN)$^-$} moiety is most likely to be present in solution, and this would react via an S$_{N}$2-type pathway through a transition state such as **TS1$_{SN2}$**. Once intermediates such as *cis*- or *trans*-[(PH$_3$)$_2$Pd(CN)Et] have been formed, subsequent PH$_3$/CN$^-$ substitution to give *cis*-[(PH$_3$)Pd(CN)$_2$-Et]$^-$ and then [Pd(CN)$_3$Et]$^{2-}$ appears to be very favorable, the solvent-corrected energies associated with these steps being −26.7 and −19.1 kcal/mol respectively.

To ensure that these conclusions are not biased by our choice of model system, we have performed a number of additional test calculations with larger model species. The energies of PPh$_3$ addition to [Me$_3$NEt]$^+$ [Pd(CN)(PPh$_3$)]$^-$ are very similar to those described above for the PH$_3$ model (solvent corrected values:

ΔE = −1.9 kcal/mol, ΔG = +12.4), and these values are virtually unchanged when the full [Bu$_3$NBu]$^+$ [Pd(CN)(PPh$_3$)]$^-$ model is considered (ΔE = −1.7 kcal/mol, ΔG = +12.1). Although it should be stressed that the effects of forming ion-pair aggregates[30] have not been taken into account in this analysis,[36] these results do suggest the dominant presence of 2-coordinate {(PR$_3$)Pd(CN)$^-$}. The C−N bond activation transition states **TS1$_{SN2}$** and **TS1$_{anti}$** have also been computed for various [(PR$_3$)Pd(CN)]$^-$/[R′NR″$_3$]$^+$ models. The results show that increased steric bulk on PR$_3$ (R = H, Ph), the reacting alkyl chain (R′ = Et, Bu), and the spectator alkyl chains (R″ = Me, Bu) all serve to reduce the preference for **TS1$_{SN2}$** over **TS1$_{anti}$**. However, even for the full [(PPh$_3$)Pd(CN)]$^-$/[BuNBu$_3$]$^+$ model, **TS1$_{SN2}$** remains over 3 kcal/mol lower in energy than **TS1$_{anti}$**. Taken together, these results suggest an intrinsic electronic preference for S$_{N}$2-type oxidative addition over E2-type Hofmann elimination in the [(PPh$_3$)Pd(CN)]$^-$/[BuNBu$_3$]$^+$ system, a preference that is counteracted to some extent by steric effects. See the Supporting Information for full details.

---

(36) Equally, we cannot preclude the possibility of further PPh$_3$/CN$^-$ substitution to form *bis*-cyano active species. To assess this, all four reaction pathways were computed for the ion pair [Pd(CN)$_2$]$^{2-}$·[Me$_3$NEt]$^+$ and a similar trend for the activation barriers (kcal/mol, after solvent correction) was computed: **TS$_{SN2}$** (+14.6) < **TS$_{syn}$** (+17.2) < **TS$_{anti}$** (+19.1) < **TS$_{conc}$** (+33.0). Full details are given in the Supporting Information. These barriers are slightly lower than those computed from *mono*-cyano **1** and reflect the greater nucleophilic/basic character of the dianionic reactant. However, the key point is again that the S$_{N}$2 process is most favorable.

Discussion

In this section, we will first discuss the two distinct mechanisms governing the two unusual C−N activation reactions of [(Ph$_3$P)$_4$Pd] with tetrabutylammonium cyanide (eqs 2 and 3). In the presence of small quantities of water, the [(Ph$_3$P)$_4$Pd]/[Bu$_4$N]$^+$ CN$^-$ system reacts to give [(CN)$_3$PdH]$^{2-}$ (eq 2), a process that involves cyanide hydrolysis to HCN in the first step. As will be shown, this non-organometallic C−N activation can be *catalytic* in H$_2$O. Under anhydrous conditions, an alternative path produces [(CN)$_3$PdBu]$^{2-}$ (eq 3) via S$_N$2-type C−N bond cleavage of [Bu$_4$N]$^+$ with mixed cyano phosphine Pd(0) species. Having discussed the C−N activation reactions, we will analyze other transformations leading to palladium catalyst deactivation during the reaction of haloarenes with cyanide (eq 1) and possible strategies on how to avoid or minimize the catalyst deactivation problem.

Mechanisms of Reactions of Pd(0) with CN$^-$ in the Presence of Moisture. With regards to palladium catalyst activity and stability, these reactions are of particular importance because practical palladium-catalyzed cyanation of aryl halides (eq 1) is seldom run under rigorously anhydrous conditions. Unless the standard organometallic Schlenk-line or drybox techniques are employed, ingress of some quantities of water into the cyanation reaction medium is almost unavoidable. Even if the substrate and the solvent are dry, a brief exposure of hygroscopic NaCN, KCN, and other ionic cyanides to air prior to use inevitably leads to the presence of water in the reaction medium. This, in turn, produces HCN due to facile hydrolysis of the cyanide anion. Our experiments demonstrate that zerovalent palladium complexes are highly reactive toward HCN. As shown in eq 5, [(Ph$_3$P)$_4$Pd] readily and irreversibly reacts with HCN that is generated upon hydrolysis of KCN in the presence of excess cyanide to produce catalytically inactive tetracyanopalladate. This reaction involves phosphino−hydrido intermediates formed via HCN oxidative addition to Pd(0), which react with another molecule of HCN and then with CN$^-$ to produce [(CN)$_4$Pd]$^{2-}$. However, at low concentrations of HCN and high enough concentrations of active cyanide the phosphine palladium hydride species can undergo facile ligand exchange to produce [(CN)$_3$PdH]$^{2-}$. This is the case when [(Ph$_3$P)$_4$Pd] is reacted with slowly added or generated HCN in the presence of excess [Bu$_4$N]$^+$ CN$^-$ (eq 4). As HCN emerges from hydrolysis to be quickly and irreversibly consumed via oxidative addition to Pd(0), hydroxide is generated in equimolar quantities. Provided the overall amount of water in the medium is small, the OH$^-$ produced is weakly hydrated. Such hydroxide is highly basic and hence can[37] easily react with the tetrabutylammonium cation to follow the classical Hofmann elimination path.[38] As a result, the amine and olefin are formed, along with a molecule of water, which can then hydrolyze another cyanide anion and so forth, thus acting as a catalyst for reaction 2 (Scheme 5).

The catalysis shown in Scheme 5 is likely the reason for the occurrence of reaction 2 in the earlier experiments[9] with the old [(Ph$_3$P)$_4$Pd] sample, which we suspect was wet (see above).[39] That would also explain why small quantities of H$_2$O intention-

Scheme 5
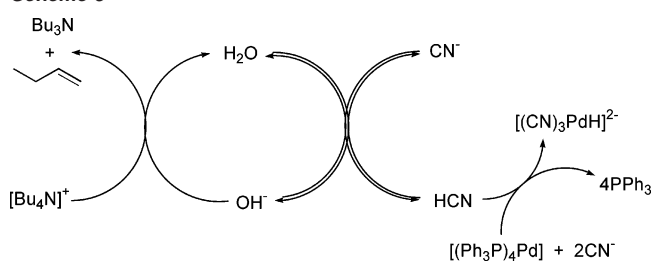
ally added to the reaction of the old sample of [(Ph$_3$P)$_4$Pd] did not seem to have a dramatic effect.[9] Furthermore, deliberate addition of H$_2$O to a solution of [Bu$_4$N]$^+$ ^{13}CN$^-$ and the newly obtained, anhydrous [(Ph$_3$P)$_4$Pd] in THF led to the formation of [(CN)$_3$PdH]$^{2-}$, whereas in the absence of water [(CN)$_3$PdBu]$^{2-}$ was exclusively produced from the same, anhydrous Pd(0) reagent under otherwise identical conditions.[39]

It is also worth noting that the amount of water in the system should be within certain limits to efficiently catalyze the reaction shown in Scheme 5. Larger quantities of water would certainly promote cyanide hydrolysis but would also inevitably result in a more hydrated form of OH$^-$ of diminished basicity, which is less capable of deprotonating [Bu$_4$N]$^+$. This explains why smaller amounts of water are particularly efficient at catalyzing reaction 2. In the presence of larger quantities of water, the palladium hydride can still be formed but the Hofmann elimination would be strongly inhibited.

Mechanisms of the Reaction of [(Ph$_3$P)$_4$Pd] with [Bu$_4$N]$^+$ CN$^-$ under Anhydrous Conditions (Eq 3). While resulting in very similar outcomes, reactions 2 and 3 are governed by totally different mechanisms. Obviously, in the absence of water, no hydroxide is produced to react with [Bu$_4$N]$^+$ via classical Hofmann degradation (Scheme 5). The results of our experimental and computational studies of the formation of [(CN)$_3$PdBu]$^{2-}$ (eq 3) are consistent with the Beringer−Gindler kinetic theory of reactions involving cations and anions in equilibrium with ion pairs which undergo irreversible decomposition.[40] This kinetic model was successfully used by Beringer's group in a series of studies of the reactions of diaryliodonium salts with charged nucleophiles.[41−43] When most of the ions are associated in ion pairs, the reaction displays first-order kinetics.[40] For instance, Ph$_2$I$^+$ reacts with Cl$^-$ to give PhI and PhCl by first-order kinetics in less ionizing DMF but by second order, and much more slowly, in strongly ionizing water.[42,44]

When [(Ph$_3$P)$_n$Pd] is treated with [Bu$_4$N]$^+$ CN$^-$, ligand exchange occurs to produce tetrabutylammonium salts of mixed cyano phosphine Pd(0) anions. In low-polar solvents, these species are expected to exist in the form of tight ion pairs

(37) Landini, D.; Maia, A.; Rampoldi, A. *J. Org. Chem.* **1986**, *51*, 3187 and 5475.

(38) (a) Hofmann, A. W. *Ann. Chem. Pharm.* **1851**, *78*, 253; *Ber. Dtsch. Chem. Ges.* **1881**, *14*, 659. (b) For an interesting review of this and closely related contributions of August Wilhelm von Hofmann, see: Alston, T. A. *Anesth. Analg.* **2003**, *96*, 622.

(39) The 99% purity stipulated by the manufacturer of the old [(Ph$_3$P)$_4$Pd] reagent allows for the presence of up to 1% of H$_2$O. A ca. 99:1 [(Ph$_3$P)$_4$Pd] to H$_2$O weight ratio translates into 30−40 mol % of water that may be present (even without any further contamination) to act as a catalyst for the hydride formation (Scheme 5). It is worth emphasizing, once again, that the PhI test performed on the old [(Ph$_3$P)$_4$Pd] sample had indicated that otherwise the reagent was pure (see above and footnote 21a). This information is provided as a cautionary note that some Pd(0) reagents, while being free from Pd(II), extra phosphine, phosphine oxide, and so forth, might still contain small quantities of water. Although in the vast majority of cases such slight contamination with water would not influence significantly the performance of the Pd(0) reagent, certain transformations can be affected dramatically, as clearly demonstrated in this work.

(40) Beringer, F. M.; Gindler, E. M. *J. Am. Chem. Soc.* **1955**, *77*, 3200.

(41) Beringer, F. M.; Gindler, E. M. *J. Am. Chem. Soc.* **1955**, *77*, 3203.

(42) Beringer, F. M.; Geering, E. J.; Kuntz, I.; Mausner, M. *J. Phys. Chem.* **1956**, *60*, 141.

(43) Beringer, F. M.; Mausner, M. *J. Am. Chem. Soc.* **1958**, *80*, 4535.

associated in clusters, like conventional quaternary ammonium salts.[30] For instance, K_D for tetrabutylammonium picrate in benzene has been estimated at only 6.5×10^{-18} (25 °C).[30b] The first-order kinetics exhibited by the reaction of $[Bu_4N]^+ CN^-$ with $[(Ph_3P)_nPd]$ is therefore in full accord with a mechanism involving the formation and collapse of an ion pair comprised of a cyano phosphine Pd(0) anion and $[Bu_4N]^+$. The extreme complexity of the $[Bu_4N]^+ CN^-/[(Ph_3P)_nPd]$/THF system stems from the aggregate,[30] solvation, and ligand-exchange (VT NMR) dynamics involved, with conceivable contributions from the rich coordination modes and uncommon bonding abilities of cyanide[47] which might bridge two metal centers by means of both σ- and π-bonding.[48] Nonetheless, the *molecular* mechanistic model below is coherent with both experimental and computational results obtained in this work.

The results of our mutually complementing experimental and computational studies are fully consistent with C−N oxidative addition rather than the Hofmann elimination/alkene insertion reaction path for C−N activation, resulting in the butyl−palladium complex (eq 3). Indeed, the exclusive formation of the linear isomer and the lack of deuterium scrambling in the reaction of $[(CH_3CH_2CD_2CH_2)_4N]^+ CN^-$ supports C−N oxidative addition rather than Hofmann elimination. Once formed, $[(CN)_3PdBu]^{2-}$ does not undergo β-elimination under the reaction conditions, that is, in the presence of extra cyanide. Accordingly, $[(CN)_3PdH]^{2-}$ does not undergo migratory insertion of olefins (ethylene, 1-butene) in the presence of free CN^- even at elevated temperatures. Furthermore, the modest KIE of ca. 1.3−1.6 observed at 20 °C for $[(C_4D_9)_4N]^+$ $^{13}CN^-$ and $[(CH_3CH_2CD_2CH_2)_4N]^+$ $^{13}CN^-$ is not necessarily in accord with C−H bond cleavage in the rate-limiting step.[49] The C−H···Pd agostic interaction found in the computational study for **TS2$_{SN2}$** (**T$_{CN}$**) and the slightly more "electropositive" character of deuterium as compared to protium (among other factors[49]) may account for the observed KIE and its magnitude. As for the intimate mechanism of the C−N oxidative addition, our computational studies point to its S_N2 rather than 3-center

Scheme 6
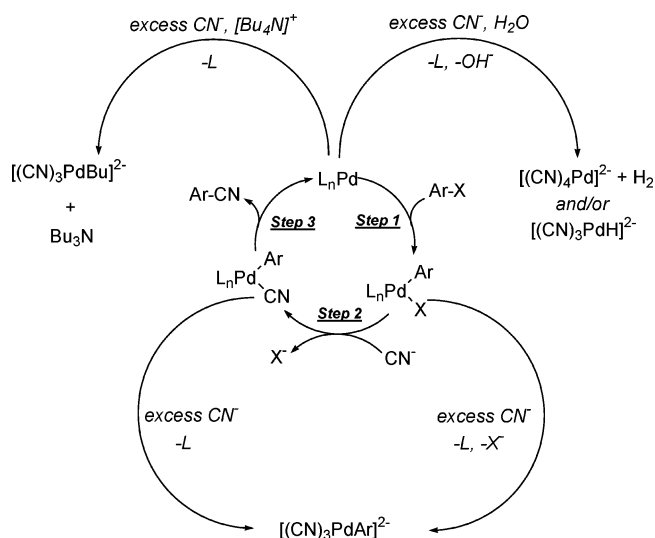
character, regardless of the composition of the mixed cyano phosphine Pd(0) anion.

A Summary of Catalyst Deactivation Paths in Palladium-Catalyzed Cyanation of Aryl Halides. Our studies reveal a number of previously unidentified reaction pathways (Scheme 6) leading to the widely acknowledged catalyst deactivation during haloarene cyanation.

In the presence of even small amounts of water, hydrolysis of cyanide occurs to generate HCN, which can compete with the ArX substrate for oxidative addition to the Pd(0) catalyst[50] and thus impair the catalysis. The beneficial effects of some bases[1,8] and HCN scavengers such as alumina[51] might be due to their ability to somewhat suppress the hydrolysis of CN^- and/or lower the concentration of HCN in the system. Depending on the current concentrations of both water and cyanide, the activity of the latter, the solvent, and temperature used, the reaction may lead to $[(CN)_4Pd]^{2-}$ (eq 5) or $[(CN)_3PdH]^{2-}$ (eq 2 and Scheme 5). Both dianions are catalytically inactive. However, reducing the Pd(II) back to Pd(0) would reactivate the catalyst. This explains why running aromatic cyanation in the presence of a reducing agent such as zinc has a tremendous beneficial effect on such parameters as turnover number and frequency, overall conversion, and yield.[52,53] The dianionic hydride $[(CN)_3PdH]^{2-}$ could also be rendered active Pd(0) via reductive elimination of HCN. This reductive elimination, however, requires predissociation of one cyano ligand to form tricoordinate $[(CN)_2PdH]^-$ and is therefore efficiently suppressed by excess cyanide in the system.

The problem of catalyst deactivation due to HCN generation from the cyanide reagent persists when the process is run in protic solvents, such as alcohols, glycols, etc. Any proton source in the catalytic system is a potential danger to the palladium catalyst due to the facile formation of HCN via protonation of

(44) Another example is the reaction of Ph_2I^+ with PhO^- to produce PhI and PhOPh.[41] While being second order in 1:1 dioxane−water favoring free ions, the reaction approached first order at higher dioxane−water ratios promoting ion pairing. Interestingly, this work could have resulted in the discovery of phase-transfer catalysis. In their publication, Beringer and Gindler wrote, "Exploratory runs showed that while the reaction in water had a convenient rate at 80°, the kinetics were complicated by the fact that the finely dispersed second phase of insoluble reaction products effected a considerable acceleration of the reaction. In a typical run a zeroth order plot is linear from about 3−70% reaction. The reaction caused by the second phase cannot be equally distributed throughout the second phase, for the bulk of this second phase increased at least 20-fold during this portion of the reaction. Possibly surface effects are operative, small drops being initially formed but coalescing to larger drops having a smaller surface-volume ratio... To maintain homogeneity, dioxane-water mixtures were used in all subsequent runs."[41] Lewis and Stout[45] also noticed that the rates of the reaction of Ph_2I^+ with aqueous hydroxide were sensitive to all second phase of PhI, Ph_2O, and other products that were forming as the reaction proceeded. Apparently, in both cases[41,45] the emerging organic phase triggered the phenomenon of phase-transfer catalysis, with the iodonium cation acting as both a reacting electrophile and a phase-transfer agent.[46]
(45) Lewis, E. S.; Stout, C. A. *J. Am. Chem. Soc.* **1954**, *76*, 4619.
(46) Grushin, V. V.; Tolstaya, T. P.; Lisichkina, I. N. *Izv. Akad. Nauk, Ser. Khim.* **1982**, 2175. Grushin, V. V.; Kantor, M. M.; Tolstaya, T. P.; Shcherbina, T. M. *Izv. Akad. Nauk, Ser. Khim.* **1984**, 2332. Grushin, V. V. *Acc. Chem. Res.* **1992**, *25*, 529 and references cited therein.
(47) Beck, M. T. *J. Indian Chem. Soc.* **1977**, *54*, 19.
(48) Our VT NMR studies of the $[Bu_4N]^+ CN^-/[(Ph_3P)_4Pd]$/THF system suggest that under certain conditions only ca. 1 equiv of coordinated PPh₃ and 1 equiv of coordinated CN^- are present per 1 equiv of palladium (Table 4, entry 4). Although it is hardly conceivable that the species observed is $[(Ph_3P)Pd(CN)]^-$, the latter might be present in small concentrations due to equilibrium with oligomeric $\{[(Ph_3P)Pd(CN)]^-\}_n$, in which the cyano ligands bridge the palladium centers.

(49) Melander, L.; Saunders, H. W., Jr. *Reaction Rates of Isotopic Molecules*; Wiley: New York, 1980.
(50) Although no quantitative data have been obtained, HCN appears to oxidatively add to $[(Ph_3P)_4Pd]$ much more easily than most reactive haloarenes, such as PhI. The difference in reactivity can be qualitatively estimated from the fact that $[(Ph_3P)_4Pd]$ reacts with PhI within minutes at room temperature, whereas the reaction of $[(Ph_3P)_4Pd]$ with HCN occurs within the time of mixing at ca. 0 °C.
(51) Dalton, J. R.; Regen, S. L. *J. Org. Chem.* **1979**, *44*, 4443.
(52) See, for example: Okano, T.; Iwahara, M.; Kiji, J. *Synlett* **1998**, 243. Okano, T.; Kiji, J.; Toyooka, Y. *Chem. Lett.* **1998**, *5*, 425.

basic cyanide. The most economical and widely used sources of cyanide for reaction 1 are KCN and NaCN. These ionic salts are hygroscopic, highly soluble in water, easily hydrolyzable, and hence most potentially poisonous to the palladium catalyst. Zinc cyanide[6] and $K_4[Fe(CN)_6]$,[7] both of which have been extensively used[1] for reaction 1, are considerably less capable of producing free CN^- and consequently deactivating the catalyst.

In practical synthesis, aromatic cyanation with KCN or NaCN is seldom run in an aprotic solvent under rigorously anhydrous conditions. The solubility of KCN and NaCN in such systems is often insufficient for the catalytic reaction to occur at a desired rate. As cyanide is lipophilic, phase-transfer catalysis might be a particularly good technique to solve this problem.[1] However, most commonly used phase-transfer catalysts are quaternary alkylammonium salts which, as we show in this work, can easily react with zerovalent palladium complexes in the presence of cyanide even under rigorously anhydrous conditions (eq 3). This leads to catalyst deactivation due to the formation of $[(CN)_3PdAlk]^{2-}$. In fact, Anderson and co-workers[54] have reported that the otherwise efficient ArX cyanation system Pd(0)/CuI/NaCN/THF lost its activity upon replacement of the NaCN with $[Bu_4N]^+$ CN^-. Therefore, crown ethers should be preferred phase-transfer catalysts for this process. It is noteworthy, however, that crown ethers are often hygroscopic and therefore may be another source of water (and hence HCN) that would ultimately deactivate the palladium catalyst due to the reactions described above. Some nonhygroscopic metal compounds capable of forming ate cyanide complexes such as Cu(I)[54−56] and Sn(IV)[57] for CN transfer to palladium have been shown to efficiently promote palladium-catalyzed aromatic cyanation with alkali metal cyanides in aprotic solvents of low polarity.

Even if all of the above-described problems dealing with catalyst deactivation prior to the Ar−X oxidative addition step are avoided by using rigorously anhydrous conditions and no quaternary ammonium salts, the process may still be terminated at steps 2 and 3 of the loop (Scheme 6).[9] The σ-aryl palladium intermediate from step 1 takes the desired path to ArCN only if no large excess CN^- is present; otherwise, R_3P/CN^- ligand exchange competes with the Ar−CN reductive elimination to give catalytically inactive $[(CN)_3PdAr]^{2-}$. Indeed, $[(Ph_3P)_2Pd(I)Ph]$ reacted with an equimolar amount of CN^- to give PhCN and Pd(0), whereas fast addition of 4−6 equiv of cyanide to the same phenyl iodo complex gave rise exclusively to stable $[(CN)_3PdPh]^{2-}$ (Scheme 2).[9] The high selectivities of these reactions, taking into consideration the detection limits (NMR), suggest that the rate constants for I^-/CN^- exchange, Ph_3P/CN^- exchange, and Ph−CN reductive elimination decrease in the order $k_{I/CN} > k_{P/CN} \geq k_{RE} \times 10^2$.[9] Therefore, if an aromatic cyanation reaction requires a phase-transfer agent, its concentration should be comparable to that of the palladium catalyst used, in order to avoid high $[CN^-]$ to $[Pd]$ ratios.

Conclusions

Mechanisms of palladium catalyst deactivation during cyanation of haloarenes (eq 1) have been for the first time identified and studied in detail. The key results of our investigations are presented in Scheme 6 showing that the process can be terminated at every step of the catalytic loop.

The presence of moisture in the reaction medium is one of the greatest dangers for the catalysis employing readily ionizable sources of cyanide that easily generate HCN upon hydrolysis. It has been demonstrated that phosphine-stabilized Pd(0) is highly reactive toward HCN, undergoing transformations to catalytically inactive $[(CN)_4Pd]^{2-}$ and/or $[(CN)_3PdH]^{2-}$. There are some ways to avoid this. Running the process under rigorously anhydrous conditions in an aprotic solvent would eliminate the problem but may be unrealistic in practice. Even if moisture is thoroughly avoided, the low solubility[3d] of alkali metal cyanides in most nontoxic aprotic solvents suitable for the catalysis, such as THF and MeCN, might require use of a phase-transfer agent. However, care is required in the choice of the phase-transfer catalyst as we have shown here that quaternary ammonium cations such as $[Bu_4N]^+$ undergo N−Alk bond cleavage with $[(Ph_3P)_nPd]$ in the presence of cyanide to give catalytically inactive $[(CN)_3PdAlk]^{2-}$. This uncommon C−N bond activation is remarkably facile, readily occurring even at room temperature and being particularly fast at low concentrations of the Pd(0). Both experimental and theoretical studies of this reaction have pointed to the involvement of mixed cyano phosphine Pd(0) anions undergoing C−N oxidative addition of the S_N2 type.

The X/CN exchange (step 2) and reductive elimination (step 3) of the loop (Scheme 6) can be easily disrupted by excess cyanide due to facile phosphine displacement with CN^-, leading to $[(CN)_3PdAr]^{2-}$. Being reluctant to undergo Ar−CN reductive elimination in the presence of extra CN^-, this dianionic palladium aryl is another dead end for the catalytic process, unless catalyst reactivation is somehow achieved, for example via reduction to Pd(0). In light of our studies, the well-known beneficial effect of a reducing agent such as zinc on palladium-catalyzed aromatic cyanation is readily accounted for by catalyst reactivation via reduction to active Pd(0) of the products of the catalyst poisoning $[Pd(CN)_4]^{2-}$, $[(CN)_3PdH]^{2-}$, $[(CN)_3PdAr]^{2-}$, and $[(CN)_3PdAlk]^{2-}$ (Alk = Bu in this work).

Finally, some conclusions drawn from our work may apply to nickel-catalyzed cyanation of aryl halides, albeit the nickel catalysis has its own characteristic features and problems.[58]

Experimental Section

Caution: Cyanides and HCN are highly toxic! All chemicals were purchased from Aldrich, Fluka, and Strem chemical companies, except $K^{13}CN$ (99% ^{13}C), n-C_4D_9I (98% D), and $CH_3CH_2CD_2CH_2Br$ (99.3% D) that were obtained from Icon Isotopes, Cambridge Isotopes, and CDN Isotopes, respectively. The solvents were dried using standard

(53) (a) The highly beneficial effect of a reducing agent on aromatic cyanation is often believed to be due to catalyst recuperation from poisoning by oxygen that is damaging to Pd(0).[53b,c] Indeed, the O_2-induced catalyst deactivation is likely the main reason to use a reductant for aromatic cyanation with $Zn(CN)_2$,[53b−d] a poorly soluble salt that is resistant to hydrolysis. However, when easily hydrolyzable KCN or NaCN is used in the presence of water, the catalyst is most efficiently poisoned by the resultant HCN which is apparently much more reactive toward Pd(0) than O_2. Our own experience with catalytic aromatic cyanation with alkali metal cyanides indicates that water can be detrimental to the catalysis even under rigorously O_2-free conditions. (b) Chidambaram, R. *Tetrahedron Lett.* **2004**, *45*, 1441. (c) Martin, M. T.; Liu, B.; Cooley, B. E.; Eaddy, J. F. *Tetrahedron Lett.* **2007**, *48*, 2555. (d) For selected reports, see: Jin, F.; Confalone, P. N. *Tetrahedron Lett.* **2000**, *41*, 3271. Ramnauth, J.; Bhardwaj, N.; Renton, P.; Rakhit, S.; Maddaford, S. P. *Synlett* **2003**, *14*, 2237. Erker, T.; Nemec, S. *Synthesis* **2004**, 23. Hatsuda, M.; Seki, M. *Tetrahedron* **2005**, *61*, 9908. Littke, A.; Soumeillant, M.; Kaltenbach, R. F., III; Cherney, R. J.; Tarby, C. M.; Kiau, S. *Org. Lett.* **2007**, *9*, 1711.
(54) Anderson, B. A.; Bell, E. C.; Ginah, F. O.; Harn, N. K.; Pagh, L. M.; Wepsiec, J. P. *J. Org. Chem.* **1998**, *63*, 8224.
(55) Allentoff, A. J.; Markus, B.; Duelfer, T.; Wu, A.; Jones, L.; Ciszewska, G.; Ray, T. *J. Labelled Compd. Radiopharm.* **2000**, *43*, 1075.
(56) For the use of CuCN as a source of cyanide in palladium-catalyzed aromatic cyanation, see: Sakamoto, T.; Ohsawa, K. *J. Chem. Soc., Perkin Trans. 1* **1999**, 2323.
(57) Yang, C.; Williams, J. M. *Org. Lett.* **2004**, *6*, 2837.

techniques and stored over freshly calcined molecular sieves (4 Å) in a glovebox. All manipulations were carried out under nitrogen in a glovebox, except as noted otherwise. NMR spectra were obtained with a Bruker Avance DRX400 and Varian Unity Inova systems operating at 400 and 500 MHz, respectively. A Bruker-CCD instrument was used for single-crystal X-ray diffraction studies. Microanalyses were performed by Micro-Analysis, Inc., Wilmington, Delaware.

Preparation of [Bu₄N]⁺ ¹³CN⁻. A mixture of [Bu₄N]⁺ OH⁻·30H₂O (4.00 g; 5 mmol), K¹³CN (0.40 g; 6.1 mmol), and THF (12 mL) was stirred under N₂ for 10 min. Anhydrous CaSO₄ in granules was added while stirring to fully absorb the small amount of the bottom aqueous phase. The THF phase was separated. The solids were thoroughly washed with THF (3 × 10 mL). All THF solutions were combined and dried with fresh anhydrous CaSO₄ under N₂ for 3 h and then filtered and evaporated under N₂. The residual oily material solidified on stirring with dry ether. After the ether was decanted off, the solid was dried under vacuum (0.01 Torr) at 30 °C for 12 h and brought to a glovebox without exposure to air. The material was dissolved in dry THF (15 mL), and the solution was vigorously stirred with powdered K¹³CN (0.10 g) for 24 h. The solution was filtered, evaporated to a viscous oil, and treated with ether. The solid was recrystallized three times from anhydrous THF−ether, dried under vacuum (0.01 Torr) at 30 °C for 60 h, and stored in the glovebox. The yield was 1.25 g (92%). ¹³C NMR (THF-d_8, 25 °C), δ: 165.0 (s).

Synthesis of [(n-C₄D₉)₄N]⁺ I⁻. A 30 mL thick-walled glass tube was charged with a magnetic stir bar, n-C₄D₉I (5.00 g; 25.9 mmol), LiOH·H₂O (0.75 g; 17.9 mmol), and MeCN (5 mL). Aqueous NH₃ (28%; 0.36 mL) was added, and the tube was immediately sealed with a Teflon-threaded stopper. The contents were vigorously stirred at 85 °C (oil bath) for 2 h, after which the tube was allowed to cool to room temperature and unsealed. The reaction mixture was treated with water (50 mL) and extracted with CH₂Cl₂ (5 × 20 mL). The combined extracts were filtered through cotton wool, and the clear, colorless filtrate was evaporated and treated with ether. The white crystals were separated, washed with ether, and dried under vacuum. The yield of [(n-C₄D₉)₄N]⁺ I⁻ was 2.00 g (92% calculated on NH₃, 76% calculated on n-C₄D₉I).

Synthesis of [(n-C₄D₉)₄N]⁺ ¹³CN⁻. A solution of NaOH (0.25 g; ca. 6.2 mmol) in water (5 mL) was added to a solution of AgNO₃ (0.51 g; 3 mmol) in water (5 mL). The precipitated Ag₂O was thoroughly washed with water and then with D₂O (5 × 2 mL). To the still wet Ag₂O was added [(n-C₄D₉)₄N]⁺ I⁻ (1.00 g; 2.5 mmol), D₂O (10 mL), and the mixture was thoroughly triturated in a mortar with a pestle for 20−30 min. After the mixture was filtered through a nylon membrane, the clear filtrate was treated with K¹³CN (0.51 g; 7.7 mmol), evaporated at room temperature under N₂ to a few milliliters, and treated with THF (100 mL). Granulated anhydrous CaSO₄ was added at stirring to absorb the water, after which the product was isolated and purified as described above for [Bu₄N]⁺ ¹³CN⁻. The yield of [(n-C₄D₉)₄N]⁺ ¹³CN⁻ was 0.65 g (86%). ¹³C NMR (THF-d_8, 25 °C, δ): 165.0 (s).

Synthesis of [(CH₃CH₂CD₂CH₂)₄N]⁺ Br⁻.[59] A 15 mL thick-walled glass tube was charged with a magnetic stir bar, CH₃CH₂CD₂CH₂Br (1.00 g; 7.2 mmol), LiOH·H₂O (0.28 g; 6.7 mmol), and MeCN (1.2 mL). Aqueous NH₃ (28%; 0.1 mL) was added, and the tube was

immediately sealed with a Teflon-threaded stopper. The contents were vigorously stirred at 85 °C (oil bath) for 24 h, after which the tube was allowed to cool to room temperature and unsealed. The reaction mixture was treated with water (10 mL) and extracted with CH₂Cl₂ (5 × 5 mL). The combined extracts were filtered through cotton wool, and the clear, colorless filtrate was evaporated and treated with ether. The white crystals were separated, washed with ether, and dried under vacuum. The yield of [(CH₃CH₂CD₂CH₂)₄N]⁺ Br⁻ was 0.51 g (97% calculated on NH₃). ¹H NMR (CD₂Cl₂, 25 °C), δ: 1.0 (t, 3H, J = 7.4 Hz, CH₃), 1.45 (q, 2H, J = 7.4 Hz, CH₂), 3.3 (s, 2H, CH₂−N).

Synthesis of [(CH₃CH₂CD₂CH₂)₄N]⁺ ¹³CN⁻. A solution of NaOH (0.15 g; ca. 3.7 mmol) in water (3 mL) was added to a solution of AgNO₃ (0.31 g; 1.8 mmol) in water (3 mL). The precipitated Ag₂O was thoroughly washed with water and then with D₂O (5 × 1 mL). To the still wet Ag₂O was added [(CH₃CH₂CD₂CH₂)₄N]⁺ Br⁻ (0.24 g; 0.7 mmol), D₂O (2 mL), and the mixture was thoroughly triturated in a mortar with a pestle for 30 min. After the mixture was filtered through a nylon membrane, the clear filtrate was treated with K¹³CN (0.11 g; 1.7 mmol), evaporated at room temperature under N₂, and treated with THF (20 mL). Granulated anhydrous CaSO₄ was added at stirring to absorb the water, after which the product was isolated and purified as described above for [Bu₄N]⁺ ¹³CN⁻. The yield of [(CH₃CH₂CD₂-CH₂)₄N]⁺ ¹³CN⁻ was 0.18 g (89%). ¹H NMR (THF-d_8, 25 °C), δ: 1.0 (t, 3H, J = 7.4 Hz, CH₃), 1.4 (q, 2H, J = 7.4 Hz, CH₂), 3.5 (s, 2H, CH₂−N). ¹³C NMR (THF-d_8, 25 °C), δ: 165.0 (s).

Preparation of H¹³CN. A 25 mL round-bottom flask was charged with a magnetic stir bar and 85% H₃PO₄ (5 mL). Finely ground K¹³CN (1.5 g; 22.7 mmol) was added at −78 °C, and the flask was immediately connected to a vacuum-transfer system, which was evacuated at ca. 0.03 mm Hg. After the Schlenk-type receiver was immersed in an acetone−dry ice bath, the H₃PO₄−K¹³CN mixture was allowed to warm to room temperature with the stirrer on. After 3 h of stirring at room temperature, the cold receiver was disconnected under N₂, evacuated, closed, and while still cold quickly brought to the glovebox, where it was allowed to warm to room temperature. Analysis of the colorless liquid (1.1 g) by ¹H and ¹³C NMR indicated that it was a solution of H¹³CN in H₂O (ca. 1:2 molar ratio). ¹H NMR (THF-d_8, 25 °C), δ: 3.2 (s, ca. 4H, H₂O), 5.4 (d, 1H, J = 260.6 Hz, H¹³CN). ¹³C NMR (¹H-decoupler off, THF-d_8, 25 °C), δ: 112.0 (d, J_{C-H} = 260.6 Hz).[23] This H¹³CN solution was stored in a tightly capped GC-MS vial placed inside a closed 20 mL scintillation vial at −25 °C inside the glovebox.

Synthesis of ([Et₄N]⁺)₂ [(¹³CN)₃Pd(H)]²⁻. To a cold (ca. 0 °C) solution of [Bu₄N]⁺ ¹³CN⁻ (145 mg; 0.5 mmol) was added [(Ph₃P)₄Pd] (220 mg; 0.2 mmol), and then, at vigorous stirring, a cold solution of the aqueous H¹³CN (see above; 20 μL) in THF (6 mL) was slowly added dropwise over the period of 15−20 min. After full discoloration, the addition of the H¹³CN solution was stopped at once. The resulting emulsion of ([Bu₄N]⁺)₂ [(¹³CN)₃Pd(H)]²⁻ in THF was homogenized by addition of 5−6 drops of MeCN. To this homogeneous mixture, a solution of [Et₄N]⁺ BF₄⁻ (78 mg) in MeCN (1.5 mL) was added at agitation. After stirring for 10 min, THF (5 mL) was added, and the cloudy mixture was kept at −20 °C overnight. The white precipitate was separated, washed with THF, and recrystallized twice from MeCN−THF. The yield of ([Et₄N]⁺)₂ [(¹³CN)₃Pd(H)]²⁻ was 73 mg (90% calculated on [Et₄N]⁺ BF₄⁻). ¹H NMR (MeCN-d_3, 25 °C), δ: −10.8 (dt, 1H, *trans*-J_{C-H} = 64.9 Hz, *cis*-J_{C-H} = 2.6 Hz, Pd−H), 1.3 (tt, 24H, J_{H-H} = 7.3 Hz, J_{N-H} = 1.9 Hz, CH₃), 3.3 (q, 16H, J_{H-H} = 7.3 Hz, CH₂). ¹³C NMR (MeCN-d_3, 25 °C), δ: 7.9 (s, CH₃), 53.3 (t, J_{N-C} = 3.2 Hz, CH₂), 137.7 (d, 2C, J_{C-C} = 5.8 Hz, mutually *trans*-CN), 146.6 (t, 1C, J_{C-C} = 5.8 Hz, CN trans to H). See also Figure 2. Anal. Calcd for C₁₆¹³C₃H₄₁N₅Pd: C, 51.5; H, 9.2; N, 15.6. Found: C, 51.4; H, 9.1; N, 14.4.

Preparation and Characterization of ([Bu₄N]⁺)₂ [(CN)₃Pd-(Bu)]²⁻. (a) A solution of [(Ph₃P)₄Pd] (24 mg; 0.02 mmol) and [Bu₄N]⁺ CN⁻ (17 mg; 0.06 mmol) in benzene (1 mL) was kept at room

(58) (a) For instance, HCN formation upon cyanide hydrolysis or solvolysis readily explains limited reproducibility[4d] of nickel-catalyzed aromatic cyanation in ethanol.[4a,b] (b) Oxidative addition of Ar−X to Ni(0) is often complicated by radical reactions[58c] and homocoupling,[58d] especially for X = I and Br. Also, Ni(0) is known[58e] to undergo Ar−CN oxidative addition, which makes the final step of the catalytic loop reversible. These features provide additional problems to nickel-catalyzed cyanation. (c) See, for example: Foa, M.; Cassar, L. *J. Chem. Soc., Dalton Trans.* **1975**, 2572. Tsou, T. T.; Kochi, J. K. *J. Am. Chem. Soc.* **1979**, *101*, 6319 and 7547. (d) See, for example: Semmelhack, M. F.; Helquist, P. M.; Jones, L. D. *J. Am. Chem. Soc.* **1971**, *93*, 5908. Amatore, C.; Jutand, A. *Organometallics* **1988**, *7*, 2203. (e) See, for example: Garcia, J. J.; Brunkan, N. M.; Jones, W. D. *J. Am. Chem. Soc.* **2002**, *124*, 9547 and references cited therein.

(59) For alternative ways of making this and other site selectively deuterated tetrabutylammonium cations, see: Heinsen, M. J.; Pochapsky, T. C. *J. Labelled Compd. Radiopharm.* **2000**, *43*, 473.

temperature for 6 days. The slightly yellow benzene solution was separated from the colorless oil, which was then washed with benzene, quickly dried, redissolved in THF-d_8, and analyzed by ^{1}H NMR (Figure 4). This experiment was repeated using [(Ph$_3$P)$_4$Pd] (124 mg; 0.11 mmol) and [Bu$_4$N]$^+$ CN$^-$ (117 mg; 0.44 mmol) in benzene (6 mL) to obtain the product in quantities sufficient for microanalysis. After washing with benzene and drying under vacuum (0.01 Torr at 30 °C for 24 h), the resultant complex in the form of a viscous, colorless oil (66 mg) retained ca. 0.5 equiv of benzene, as judged by the analytical data. Anal. Calcd for C$_{39}$H$_{81}$N$_5$Pd·0.5C$_6$H$_6$: C, 65.9; H, 11.1; N, 9.2. Found: C, 65.9; H, 11.2; N, 9.4. (b) The experiment was repeated using [Bu$_4$N]$^+$ ^{13}CN$^-$ to obtain the ^{13}C NMR spectrum shown in Figure 5. (c) After the reaction of [(Ph$_3$P)$_4$Pd] with [(CH$_3$CH$_2$CD$_2$CH$_2$)$_4$N]$^+$ CN$^-$ used in the kinetic study (Table 3) had gone to completion, NMR characterization of the reaction products was carried out using a combination of TOCSY and HMBC. The reaction components identified in this way are assigned as [(^{13}CN)$_3$PdCH$_2$CD$_2$CH$_2$CH$_3$]$^{2-}$ C(1) 8.75/1.11 (δ ^{13}C/δ ^{1}H), C(2) 36.77 (δ ^{13}C only), C(3) 29.02/1.31, C(4) 14.74/0.86, CN (trans) 147.59, CN (cis) 143.86; [(CH$_3$CH$_2$CD$_2$CH$_2$)$_4$N]$^+$ C(1) 59.40/3.53, C(2) 24.32 (δ ^{13}C only), C(3) 20.40/1.50, C(4) 14.12/1.03; and (CH$_3$CH$_2$CD$_2$CH$_2$)$_3$N C(1) 54.64/2.35, C(2) 29.87 (δ ^{13}C only), C(3) 21.12/1.32, C(4) 14.24/0.91.

Reaction of [(Ph$_3$P)$_4$Pd] with [Bu$_4$N]$^+$ ^{13}CN$^-$ in THF under Vacuum. (a) Immediately after a mixture of [(Ph$_3$P)$_4$Pd] (35 mg; 0.03 mmol) and [Bu$_4$N]$^+$ ^{13}CN$^-$ (32 mg; 0.12 mmol) was dissolved in THF (2 mL), the resulting solution was separated into two halves of 1 mL each. One of the portions was placed in a 20 mL vial and kept undisturbed inside the drybox. The other half was placed in a freshly flame-dried 6 mL glass tube equipped with a Teflon-coated magnetic stirbar, stoppered with a high-vacuum glass stopcock, and brought out of the drybox. The tube was immediately evacuated at −196 °C and after two freeze−pump−thaw cycles flame-sealed under vacuum (<0.001 Torr at −196 °C). The mixture was warmed up to room temperature and vigorously stirred. Full discoloration was observed after ca. 1.5 days. Both mixtures remained *homogeneous* throughout the reaction. Analysis of the mixtures by ^{1}H and ^{13}C NMR in MeCN-d_3 after evaporation of the THF solvent indicated that both reactions produced [(^{13}CN)$_3$PdBu]$^{2-}$ and no observable quantities of [(^{13}CN)$_3$PdH]$^{2-}$. (b) After a mixture of [(Ph$_3$P)$_4$Pd] (38 mg; 0.03 mmol) and [Bu$_4$N]$^+$ ^{13}CN$^-$ (35 mg; 0.13 mmol) was dissolved in THF (2 mL), the resulting solution was separated into two halves of 1 mL each. One of the portions was placed in a 20 mL vial and kept undisturbed inside the drybox. The other half was placed in a 50 mL round-bottom flask (that had not been flame-dried), equipped with a Teflon stopcock, brought out of the glovebox, cooled to −196 °C, and evacuated at 0.015 Torr. The still cold flask was stopcock-sealed under vacuum, after which it was warmed up to room temperature, brought back to the glovebox, and vigorously stirred. Full discoloration was observed after 1 day for the agitated reaction mixture under vacuum and after 2 days for the reaction at normal pressure. At full conversion, the mixture produced by the reaction under vacuum was a biphasic liquid−liquid system, whereas a homogeneous mixture resulted from the reaction under normal pressure. Analysis of the reaction mixtures by ^{13}C NMR in MeCN-d_3 after evaporation indicated that the undisturbed reaction at normal pressure produced [(^{13}CN)$_3$Pd(Bu)]$^{2-}$ as the main product and <1% of [(^{13}CN)$_3$Pd(H)]$^{2-}$, whereas the reaction under vacuum led to both [(^{13}CN)$_3$Pd(Bu)]$^{2-}$ and [(^{13}CN)$_3$Pd(H)]$^{2-}$ in a ca. 1:1 ratio.[20b]

Reaction of [(Ph$_3$P)$_4$Pd] with KCN in the Presence of Water. A solution of [(Ph$_3$P)$_4$Pd] (29 mg; 0.025 mmol) in THF (1.5 mL) was prepared. The ^{31}P NMR spectrum of this solution was recorded to exhibit a broadened singlet at (14.6 ppm, $\Delta\nu_{1/2}$ = ca. 70 Hz), in full accord with the literature data. To this solution was added K^{13}CN (32 mg; 0.48 mmol) as a fine powder, and the mixture was stirred under N$_2$ for 2 h. This resulted in neither color change nor any observable reaction, as judged by ^{31}P NMR of the yellow THF solution over the white solid of the K^{13}CN. N$_2$-saturated D$_2$O was added via syringe at

vigorous stirring in portions of 30, 20, and 20 μL within 5 min. The yellow color faded, and full discoloration was observed after ca. 10 min of agitation, pointing to the disappearance of Pd(0). The colorless THF solution was separated from the viscous droplets of the aqueous/inorganic phase and analyzed by ^{31}P NMR to indicate the presence of only free PPh$_3$ (s, −5 ppm). Analysis of the inorganic phase in D$_2$O (0.7 mL) by ^{13}C NMR revealed the presence of only two CN-containing species, free ^{13}CN (s, 165.6 ppm) and [Pd(^{13}CN)$_4$]$^{2-}$ (s, 131.4 ppm).

Reaction of [(Ph$_3$P)$_4$Pd] with H^{13}CN. The aqueous H^{13}CN (see above; 2.5 μL) was added to a solution of [(Ph$_3$P)$_4$Pd] (16 mg; 0.014 mmol) in THF-d_8 (0.8 mL) placed in a 5 mm NMR tube. NMR spectra of the solution were recorded 10 min after sample preparation. In the ^{1}H NMR spectrum, a hydrido resonance was observed (−8.7 ppm, d, J_{H-C} = 56.2 Hz), along with the doublet resonance from H^{13}CN (5.2 ppm, d, J_{H-C} = 261.0 Hz),[23] and a weak resonance from the already formed H$_2$ (4.5 ppm, s). In the ^{13}C NMR spectrum, the cyano hydride resonated at 141.5 ppm as a singlet and a doublet (J_{H-C} = 56.2 Hz) with the proton decoupler on and off, respectively. In addition to this signal and four resonances from PPh$_3$, the ^{13}C NMR spectrum also displayed an intense doublet from H^{13}CN (111.5 ppm, J_{H-C} = 261.0 Hz).[23] The ^{31}P NMR spectrum displayed only one broad singlet (14.5 ppm, $\Delta\nu_{1/2}$ = 150 Hz). The hydride is formulated as *trans*-[(Ph$_3$P)$_2$-Pd(H)(CN)] in fast exchange with free PPh$_3$ (resulting in loss of H−P coupling, see above), which is known to be the case with analogous hydrido cyano nickel complexes stabilized by tertiary phosphines and phosphites.[24] As the reaction occurred, H$_2$ was produced and well-shaped colorless crystals of X-ray quality formed after several hours, which were identified as *trans*-[(Ph$_3$P)$_2$Pd(CN)$_2$] by NMR and X-ray analysis. NMR data for the precipitated crystals of *trans*-[(Ph$_3$P)$_2$Pd-(^{13}CN)$_2$] (CD$_2$Cl$_2$, 25 °C), δ: ^{1}H: 7.5 (m, 12H, *m*-Ph), 7.55 (m, 6H, *p*-Ph), 7.75 (m, 12H, *o*-Ph); ^{13}C: 130.8 (t, J_{C-P} = 15.5 Hz); ^{31}P: 24.8 (t, J_{C-P} = 15.5 Hz).

Kinetic Measurements and VT NMR Studies. One-dimensional ^{13}C NMR and kinetic data were acquired on a Varian Unity Inova system operating at 500 MHz. Chemical shift referencing was obtained by setting the downfield THF solvent peak to 67.4 ppm. For convenience, the kinetic data were obtained by placing the transmitter at 150 ppm (between the [Bu$_4$N]$^+$ ^{13}CN$^-$ starting material and [(^{13}CN)$_3$Pd(Bu)]$^{2-}$ product) and restricting the spectral width to 8 kHz. An acquisition time of 2 s was used in conjunction with a recycle delay of 6 s and a 90° pulse width. Typical signal averaging involved 64 transients for a total acquisition time of approximately 8 min for each kinetic time point. The activation enthalpy ($\Delta H^{\ddagger}$) and entropy ($\Delta S^{\ddagger}$) were determined by direct nonlinear least-squares fitting of these parameters to the Eyring equation ($k_1 = (k_B T/h) \exp(\Delta S^{\ddagger}/R) \exp(-\Delta H^{\ddagger}/RT)$) using the temperature and rate constant data in Table 2. This fitting procedure gave the parameter estimates (25 °C) $\Delta G^{\ddagger}$ = 22.7 ± 0.1 kcal mol^{-1}, $\Delta H^{\ddagger}$ = 26.3 ± 0.7 kcal mol^{-1}, $\Delta S^{\ddagger}$ = 12 ± 2 cal mol^{-1} deg^{-1}, and E_a = 26.9 ± 0.7 kcal mol^{-1}. The stated uncertainties represent 95% confidence limits and were obtained using an estimated error in temperature of 2 °C and an estimated error in the rate constants as obtained from exponential fitting of the raw kinetic data. Conditions for low-temperature ^{31}P and ^{13}C NMR studies (Table 4) were established from T1 relaxation measured at −70 °C by inversion recovery experimentation. In each case, to ensure accurate integration, the total recycle time was set to 7.5 s, >5 times the longest measured T1 of 1.3 s, with inverse-gated decoupling to suppress NOE and a 45° pulse width.

Crystallographic Studies. A summary of the crystallographic data for ([Et$_4$N]$^+$)$_2$ [(CN)$_3$Pd(H)]$^{2-}$, [K·18-crown-6]$^+$ [(Ph$_3$P)Pd-(CN)(O$_2$)]$^-$, [Et$_4$N]$^+$ CN$^-$, and *trans*-[(Ph$_3$P)$_2$Pd(CN)$_2$] is given in Table 5. The CIF files are presented in the Supporting Information section.

Computational Details. All DFT calculations were run with *Gaussian 03*[60] and employed the BP86 functional. Lanl2dz pseudopo-

(60) Frisch, M. J.; et al. *Gaussian 03*, revision C.02; Gaussian, Inc.: Wallingford, CT, 2004.

Table 5. Summary of Crystallographic Data for ([Et$_4$N]$^+$)$_2$ [(CN)$_3$Pd(H)]$^{2-}$, [K·18-crown-6]$^+$ [(Ph$_3$P)Pd(CN)(O$_2$)]$^-$, [Et$_4$N]$^+$ CN$^-$, and *trans*-[(Ph$_3$P)$_2$Pd(CN)$_2$]

	([Et$_4$N]$^+$)$_2$ [(CN)$_3$Pd(H)]$^{2-}$	[K·18-crown-6]$^+$ [(Ph$_3$P)Pd(CN)(O$_2$)]$^-$	[Et$_4$N]$^+$ CN$^-$	[(Ph$_3$P)$_2$Pd(CN)$_2$]
empirical formula	C$_{19}$H$_{41}$N$_5$Pd	C$_{35}$H$_{47}$KNO$_9$PPd	C$_{27}$H$_{60}$N$_6$	C$_{38}$H$_{30}$N$_2$P$_2$Pd
FW	445.97	802.21	468.81	682.98
cryst color	colorless	colorless	colorless	colorless
form	square prism	needle	irregular block	irregular block
cryst system	monoclinic	monoclinic	monoclinic	triclinic
space group	$P2(1)/c$	$P2(1)/c$	$P2(1)/n$	P$\bar{1}$
a (Å)	19.696(4)	11.550(3)	12.025(3)	9.1134(8)
b (Å)	8.3139(16)	8.4259(19)	20.710(4)	9.7354(8)
c (Å)	14.012(3)	38.732(8)	14.224(3)	10.2226(9)
α (deg)	90	90	90	110.8770(10)
β (deg)	96.275(2)	96.543(4)	123.980(14)	93.0840(10)
γ (deg)	90	90	90	108.0970(10)
V (Å^3)	2280.7(8)	3744.8(15)	2937.4(11)	791.57(12)
Z	4	4	4	1
density (g/cm^3)	1.299	1.423	1.06	1.433
abs μ (mm^{-1})	0.825	0.701	0.063	0.717
F(000)	944	1664	1056	348
cryst size (mm^3)	0.50 × 0.18 × 0.18	0.38 × 0.08 × 0.02	0.32 × 0.32 × 0.27	0.24 × 0.24 × 0.20
T (°C)	−100	−100	−100	−100
scan mode	ω	ω	ω	ω
detector	Bruker-CCD	Bruker-CCD	Bruker-CCD	Bruker-CCD
θ_{max} (deg)	28.32	27.18	26.37	28.33
no. observed refs	29 852	35 613	35 142	12 835
no. unique refs	5672	8311	5992	3903
R_{merge}	0.038	0.092	0.064	0.031
no. params	238	421	317	198
R indices[$I > 2\sigma(I)$]^a	wR2 = 0.055, R1 = 0.024	wR2 = 0.111, R1 = 0.054	wR2 = 0.168, R1 = 0.062	wR2 = 0.062, R1 = 0.025
R indices (all data)^a	wR2 = 0.059, R1 = 0.030	wR2 = 0.131, R1 = 0.106	wR2 = 0.195, R1 = 0.094	wR2 = 0.063, R1 = 0.027
S^b	1.06	1.06	1.05	1.07
max diff peak, hole (e/Å^3)	0.31, −0.43	0.72, −0.71	0.68, −0.28	0.96, −0.43

^{a} R1 = $\sum||F_o| - |F_c||/\sum|F_o|$, wR2 = $\{\sum[w(F_o^2 - F_c^2)^2]/\sum[w(F_o^2)^2]\}^{1/2}$ (sometimes denoted as R_w2). ^{b} GOF = $S = \{\sum[w(F_o^2 - F_c^2)^2]/(n - p)\}^{1/2}$, where n is the number of reflections, and p is the total number of refined parameters.

tentials and basis sets were used for palladium and phosphorus[61] with an additional set of d-orbital polarization functions on P ($\zeta = 0.387$).[62] For the [(PH$_3$)$_n$Pd(CN)]$^-$/[EtNMe$_3$]$^+$ model ($n = 1, 2$), 6-31G** basis sets were used for all other atoms.[63] For the larger model systems, [(PPh$_3$)$_n$Pd(CN)]$^-$/[R'NR''$_3$]$^+$, R' = Et, Bu; R'' = Me, Bu, additional substituent carbon and hydrogen atoms were described with a 6-31G basis set. All gas-phase optimized stationary points were fully characterized via analytical frequency calculations as either minima (all positive eigenvalues) or transition states (one imaginary eigenvalue), and IRC calculations were used to confirm the minima linked by each transition state. Relative energies quoted in the text incorporate a number of different terms. Standard gas-phase energies include a correction for zero-point energies. A solvent correction is then added to incorporate stabilization arising from solvent polarity (THF, $\epsilon = 7.58$) as calculated via the polarized continuum model (PCM) approach.[64] Finally, the $T\Delta S$ term (298.15 K, 1 atm) derived from the gas-phase frequency calculations was included to give the solvent-corrected free energies given in the text. To check the strategy of applying a single-point PCM correction to a gas-phase optimized geometry, a number of stationary points were fully optimized, incorporating the PCM solvation effect. These test calculations showed that the computed energetics of C−N activation to be unaffected, and full details are given in the Supporting Information. Computed charges mentioned in the text are derived from a Mulliken population analysis.

Supporting Information Available: Full ref 60 and further details of computational, KIE (PDF), and crystallographic (CIF) studies. This material is available free of charge via the Internet at http://pubs.acs.org.

JA078298H

(61) Hay, P. J.; Wadt, W. R. *J. Chem. Phys.* **1985**, *82*, 299.
(62) Höllwarth, A.; Böhme, M.; Dapprich, S.; Ehlers, A. W.; Gobbi, A.; Jonas, V.; Köhler, K. F.; Stegmann, R.; Veldkamp, A.; Frenking, G. *Chem. Phys. Lett.* **1993**, *208*, 237.
(63) (a) Hehre, W. J.; Ditchfield, R.; Pople, J. A. *J. Chem. Phys.* **1972**, *56*, 2257. (b) Hariharan, P. C.; Pople, J. A. *Theor. Chim. Acta* **1973**, *28*, 213.
(64) Cancès, M. T.; Mennucci, B. B.; Tomasi, J. *J. Chem. Phys.* **1997**, *107*, 3032.